UiT
THE ARCTIC UNIVERSITY OF NORWAY

Faculty of Science and Technology

Department of Geoscience

Shallow Stratigraphic Cores NW of Bjørnøya, results and implications.

—

Isak Eikelmann

GEO-3900 Master's thesis in Geology
May 2017

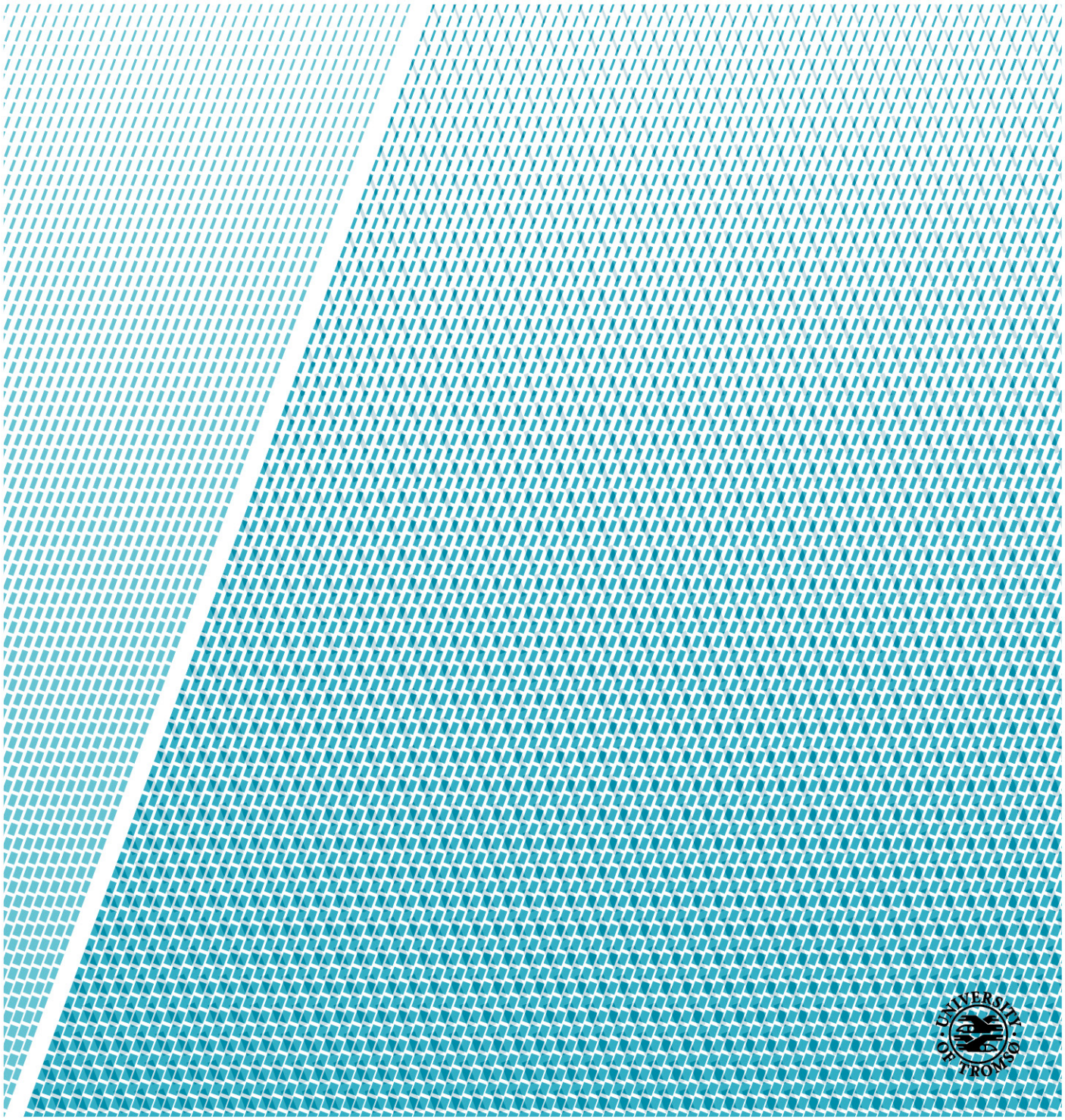

Abstract

Two shallow boreholes, 7418/01-U-01 and 7517/12-U-01, were in 1994 drilled by IKU / SINTEF on behalf of the Norwegian Petroleum Directorate (NPD) northwest of Bjørnøya in the western Barents Sea. These were part of a program totalling nine boreholes at six different locations between Bjørnøya and Svalbard. This area is not opened for petroleum activity, and the shallow boreholes were aimed at providing new data and increased geological knowledge.

The two drill sites are located were reflections are subcropping below the late Neogene and Quaternary overburden, and in two different sub-basins within the Hornsund fault complex. Borehole 7418/01-U-01 was drilled at a water depth of 181.5m. Total depth from seabed was 126.15m and 113.3m of cores were cut. Borehole 7515/12-U-01 was drilled at a water depth of 156m. Total depth from seabed was 200m and 87.8m of cores were cut.

Borehole 7418/01-U-01 penetrates Late Paleocene to Early Eocene strata, while borehole 7517/12-U-01 penetrates Late Paleocene strata. The cores show a diverse set of sedimentary features, ranging from primary depositional structures to detrimental bioturbation.

The cores are dated to Paleogene age and show a variety of sedimentary features such as ample bioturbation, ripples and various cross stratifications. The lithology varies from mud to several sandy intervals and thinner beds of conglomerate.

The findings indicate a deep marine setting for core 7418/01-U-01 and a shallow marine setting for 7517/12-U-01. This suggests that core 7418/01-U-01 correlate to the deep marine paleoenvironment to the south, while core 7517/12-U-01 correlates to the shallow marine paleoenvironment of Svalbard.

Acknowledgment

This thesis was made possible by the Norwegian Petroleum Directorate

Jeg vil gjerne takke Stig-Morten Knutsen og Iver Martens som har gjort denne oppgaven mulig for meg. Deres veiledning har vært uvurderlig.

Takk til Jan Sverre Laberg og Amando Lasabuda, for veiledning og samtaler.

En varm takk til alle nye venner jeg har fått her på instituttet. Dere har gjort studietiden til en fornøyelig opplevelse.

En takk går ut til familien min som har støttet meg, gitt meg råd og hørt på klagingen min gjennom denne tiden.

Til sist en takk til Iselin som har passet på meg og gitt meg ro i en ellers stressende hverdag, og som har oppmuntret meg til å gi alt.

Tromsø 2017-05-15

Isak Eikelmann

Table of Contents

1 Introduction

1.1 Project presentation

The focus of this thesis are two cores located north-west of Bjørnøya, at 74°52'33.3" N, 18°5'48.8" E and 75°14'16.4" N, 17°44'59.2" E, as indicated by Figure 3. The study area is located between two paleo structures, Stappen High and Hornsund Fault Complex. The cores are extracted from two sub-basins of the Knølegga Fault, which in itself is a part of the Horsund Fault Complex.

1.1.1 Objective

Extensive work has been done both in the Barents Sea South area and the in the Svalbard Archipelago area by multiple authors over a timespan of several decades. Despite this work, the Cenozoic era is still a widely discussed period of time of the evolution of the Barents Sea Shelf. In addition to the ongoing discussion about the shelf evolution, the northern Barents Sea shelf is less understood than the aforementioned southern Barents Sea shelf and Svalbard archipelago due to the area not being open for hydrocarbon exploration and generally less accessible than Svalbard. The Norwegian Petroleum Directorate is one of the primary investigators of the area.

The purpose of this thesis is to expand on the current understanding of the northern Barents Sea Shelf, by analysing and interpreting the two chosen cores. From these cores the paleo environment can be interpreted and a comparison to previous works can be done. In doing so the goal is to add to the current information and if necessary challenge pre-set notions. The following goals are set for the thesis:

- Description of both cores
- Divide the cores into sections depending on sedimentological trends
- Interpret the sedimentary textures, structures and facies
- Determine depositional environment
- Discuss the findings and compare to existing literature
- Present a regional interpretation based on the findings and existing literature

2 Study Area

The study area is located along the western margin of the Barents Sea. The geology of the area is defined by two structural elements, Stappen High and Hornsund Fault Complex. The cores are extracted from two sub-basins of the Knølegga Fault, which in itself is a part of the Hornsund Fault Complex.

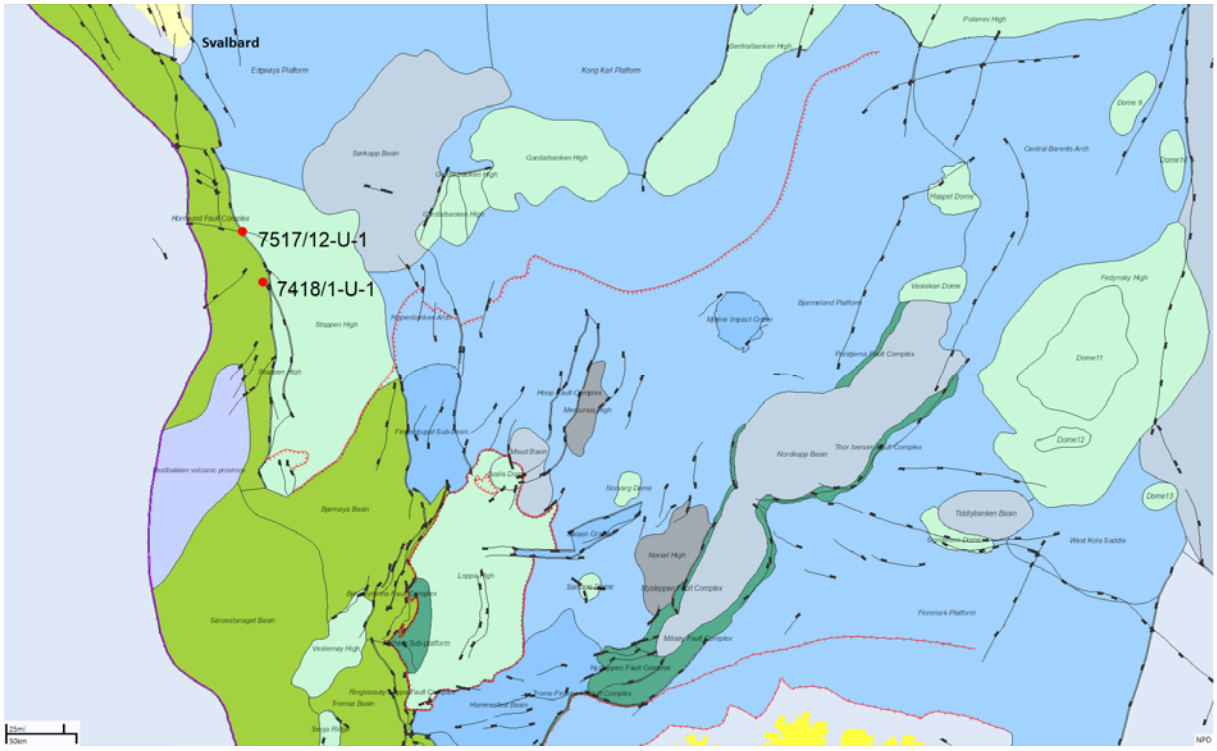

Figure 1: Map of the Barents Sea showing the main geological structures. The two boreholes used in this thesis are marked in red. (NPD, 2017)

2.1 The Barents Sea

The Barents Sea covers an extensive shelf area that stretches from the Svalbard and Franz Josef Land archipelagos in the north to the coast of Norway and Russia in the south. It is bound by the North Atlantic continental margin and the Norwegian Sea in the west and by Novaya Zemlya and the Kara Sea in the east (Grogan et al. 1999). The Barents Sea covers an area of 1.3 million km^2, 310 000 km^2 which is prospective sedimentary basins (Doré 1995, Grogan et al. 1999, Henriksen et al. 2011). The average water depth in the Barents Sea is 300m (Doré 1995).

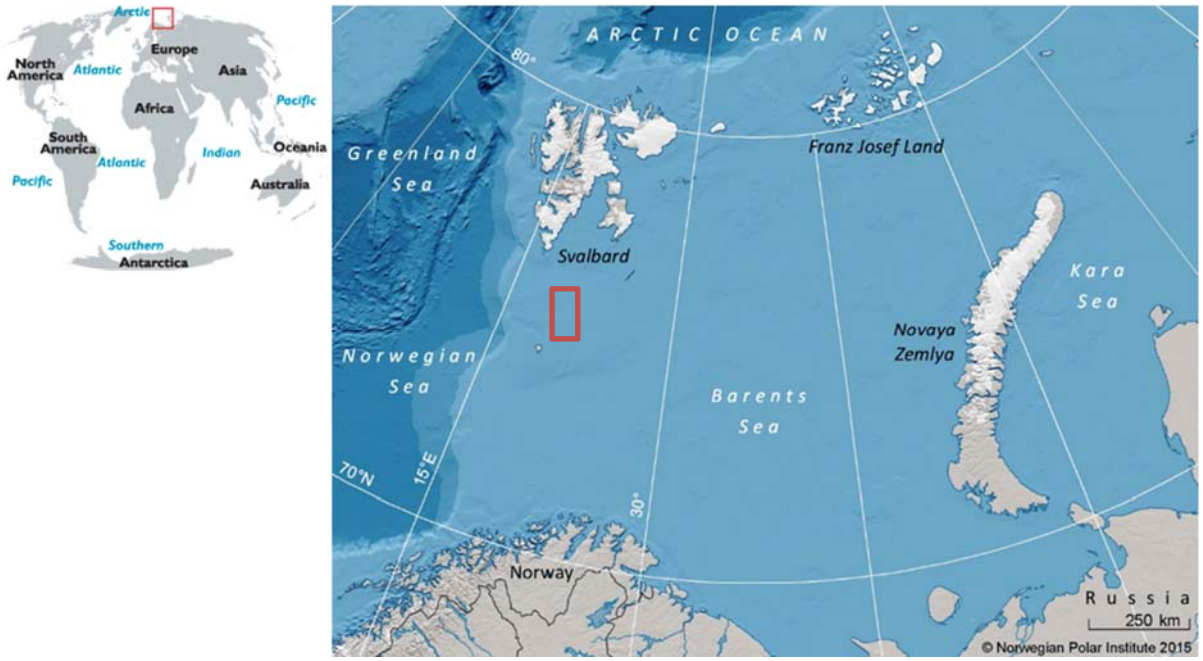

Figure 2: World map showing the location of the Barents Sea, with the study area marked in red. (Andersen et al. 2016)

Current topography of the Barents Sea is in large parts influenced by the topography of the underlying bedrock, but also shaped by the Late Cenozoic glaciation. The topography is mainly flat banks, with separating troughs in between. The troughs are especially prominent along the western margin with the Bjørnøya Trough being a prime example (Faleide et al. 1996). The western margin slopes gently between 1° and 4°, and varies in width in an N-S direction. The difference in width is caused by uneven spreading from the Knipovich Ridge (Faleide et al. 1996).

The Barents Sea can be divided into three distinct structural provinces as shown in Figure 3. South and East of Svalbard platform areas with underlying sequences of Devonian to Cretaceous age are dominating. The Western Barents Sea Margin is bounded by the deep ocean basins in the west, and separated by the platform areas by the major fault complexes of the Atlantic Ocean Basin Margin (Grogan et al. 1999). This province consists of Mesozoic and Cenozoic sub-basins southwest, west and north of Svalbard. To the east and southeast of this is the platform areas with mainly Mesozoic rocks (Grogan et al. 1999).

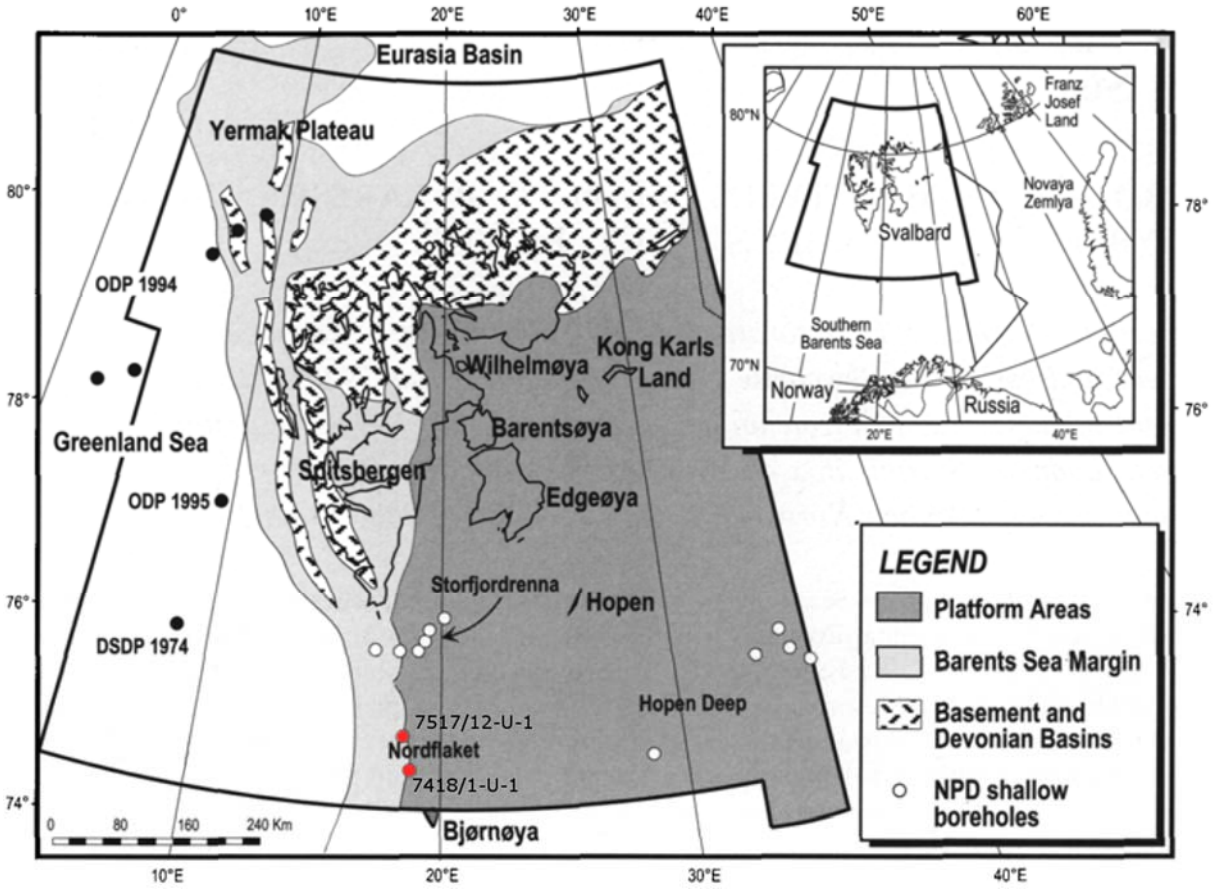

Figure 3: Map showing the three main structural provinces of the Barents Sea. The two boreholes used in this thesis are marked in red.

2.2 The Western Margin

The Western Barents Sea Margin Stretches from 70°N to 82°N and encompasses the continental margin of the Barents Sea and Svalbard as well as the Yermak Plateau (Grogan et al. 1999, Faleide et al. 2008). The margin is a structurally complex basin province. It was formed during the break-up of the supercontinent Pangea and the following seafloor spreading during the Late Mesozoic and Cenozoic (Grogan et al. 1999). It can be divided into three regions according to the successions from Upper Paleozoic to Cenozoic. The northernmost region is the Svalbard Platform 70-72°30' N, the middle section is the basin province between the Svalbard Platform and the Norwegian coast 72°30'-75° N, and the continental margin 75-80° N (Faleide et al. 1993). The continental margin region can be further divided into three sections, the southernmost shear margin associated with the Senja Fracture Zone, the central rifted complex south-west of Bjørnøya, and the northern section associated with the Hornsund Fault Zone. The Transition between ocean and continent is narrow and covered by a thick wedge from the upper Cenozoic (Faleide et al. 1993). The area along the margin west of Stappen High is comprise of isolated sub-basins that are separated by west-northwest trending lineaments. These sub-basins

are the result of reactivation of the fracture zones that originated from the rifting between Greenland and Spitsbergen (Grogan et al. 1999).

2.3 Structural Elements

Some of the structural elements important to this study are presented and described below.

2.3.1 Stappen High

Stappen High is trending north-south and is bound by the Bjørnøya Basin to the south, the Sørkapp Basin to the east, and the Knølegga Fault to the west (Gabrielsen et al. 1990). The high stretches from 73°30' N to of 75°30' N, and between 18° E and 19° E. The island of Bjørnøya, which measures 178 km^2 and is located at 74°30′N, 19°00′E, defines the highest point of the Stappen High. The seismic data from the area is generally of poor quality, and so the structure is not well mapped (Gabrielsen et al. 1990, Evenset et al. 2004).

The Stappen High has a complex tectonic history with many phases of uplift and tilting. These tectonic events have led to a severely condensed Late Paleozoic and Mesozoic succession (Grogan et al. 1999). During the Late Paleozoic, the Stappen High was a positive element until parts of the high subsided in the Early Cretaceous. The exact timing is not known, but during Cenozoic the high was once again uplifted. The Cretaceous subsidence and Cenozoic uplift is related to activity along the Knølegga Fault in the Hornsund Fault Complex, which is in turn associated with the opening of the Norwegian-Greenland Sea (Wood et al. 1989, Gabrielsen et al. 1990).

2.3.2 Hornsund Fault Complex

The Hornsund fault complex feature is not formally defined due to a lack of seismic control in the area (Gabrielsen et al. 1990). The complex is located between 73°30' N and 77° N and between 17°30' E and the ocean-continent boundary (Gabrielsen et al. 1990). To the south is the Vestbakken Volcanic Province, and the Stappen High defines the eastern delimitation. The northern boundary is not well defined. To the west, the ocean-continent boundary is the defining boundary, and it is also included in the Hornsuned fault complex (Gabrielsen et al. 1990).

The Hornsund fault complex is classified as a first class fault system. A first class fault system has basement involvement, is regionally significant, reactivated, and has separate areas of different tectonic outline. The complex is a narrow zone of down faulted blocks initiated in Early Paleocene and its genesis is associated with the opening of the Norwegian-Greenland

Sea. The complex has a dextral strike-slip displacement with an N-S trend in the southern parts and a NW-SE trend in the northern parts (Gabrielsen 1984, Eldholm et al. 1987, Gabrielsen et al. 1990). Comparing the trends of the complex with fault trends of Cenozoic and earlier age on Spitsbergen suggests that the Cenozoic rifting was constrained by deep-rooted pre-existing lineaments that stems back to Early Carboniferous (Myhre et al. 1982, Bergh et al. 2003).

2.3.3 Knølegga Fault

The Knølegga Fault separates the Hornsund Fault complex and the Stappen High. It stretches from 73°30' N to 75°50' N in a NNE-SSW to N-S trend. It is located at approximately 18°E (Gabrielsen et al. 1990). The fault is believed to be a listric fault where the detachment is at 6km depth, at Jurassic or deeper level. The throw is currently unknown, as the upthrown side exposes Jurassic crop out while at the downthrown side the Jurassic package is at an unknown depth of at least 3-4km (Gabrielsen et al. 1990). The southern termination is a structurally complex area southwest of Stappen High, while the northern termination happens at approximately 75°50' N where there is a change in orientation and deformation style (Gabrielsen et al. 1990). The Knølegga Fault is believed to be a primarily extensional feature, but movement during Cenozoic may have had a lateral component, believed to be dextral (Gabrielsen et al. 1990).

3 Geological Evolution

3.1 Structural Development

The Barents Sea has a long and complex evolutionary history with several tectonic events, and periods of uplift and subsidence that is mirrored by the geology we observe today. There are five phases of basement development that are widely accepted; 1) Late Devonian - Middle Carboniferous rifting, 2) Late Carboniferous - Permian carbonate platform development, 3) Triassic - Cretaceous siliciclastic shelf development, 4) Early Cenozoic crustal break-up, and 5) Late Cenozoic passive margin development (Ryseth et al. 2003).

3.1.1 Cretaceous

In Late Jurassic - Early Cretaceous time the northeast Atlantic-Arctic rift episode resulted in thinning of the crust, which lead to the formation some of the main basins in the Western Barents Sea: the Harstad-, Tromsø-, Bjørnøya- and Sørvestnaget Basins. Following the thinning, rapid differential subsidence occurred and the basins experienced segmentation into sub-basins and highs. There is evidence for a phase of Middle Cretaceous extension confined mainly to the southwestern Barents Sea. Towards the end of the Mesozoic, regional uplift in the north led to southward sediment progradation (Brekke et al. 2001, Faleide et al. 2008).

Towards the end of the Cretaceous period rifting and extension between Europe and Greenland occurred as a consequence of the breakup of the super continent Pangea. Within the de Geer Zone there were strike-slip movement between Norway and Greenland, resulting in extension and pull-apart basins forming in the southwestern parts of the Barents Sea (Faleide et al. 2008). The DeGeer Zone is made up of the Senja Fracture Zone, Hornsund Fault Zone and Greenland Fracture Zone. It is a broad dextral regional shear zone separating Svalbard and northeasern Greenland (Blinova et al. 2009). The final rift episode started in Maastrichtian, Late Cretaceous (Skogseid et al. 2000, Faleide et al. 2008). As a result of the rifting a dextral stress field was set up along the Senja Lineament and Hornsund Lineament (Smelror et al. 2009).

3.1.2 Paleocene

Into the Early Paleocene the ridge system progrades north along the Spitsbergen Shear Zone to form the Knipovich Ridge (Ritzmann et al. 2002). During the Paleocene period a short-lived change in spreading direction in the Labrador Sea, west of Greenland, led to transpression along the Hornsund Lineament (Bergh et al. 2003, Ritzmann et al. 2003). This transpression led to the Spitsbergen Orogeny (Ritzmann et al. 2002). Towards the Late Paleocene-Eocene transition final lithospheric breakup occur (Skogseid et al. 2000, Brekke et al. 2001, Faleide et al. 2008).

The breakup is associated with a 3-6 m.y. period of massive magmatic activity (Faleide et al. 2008). Following the final breakup there was a regional uplift, which cause is unknown (Brekke et al. 2001).

3.1.3 Eocene

The seafloor spreading between Greenland and the Barents Sea happened in an oblique fashion. The initiation of seafloor spreading in the southern parts started in the Early Eocene (Smelror et al. 2009). At this time Greenland started to move as a separated plate causing oblique movement to the western Spitsbergen. This oblique movement caused the main compressive deformation within the West Spitsbergen Fold Belt system (Blinova et al. 2009). Oblique-slip movement along this orogenic belt caused the formation of the Svalbard Central Basin, which is a main basin for tertiary deposition (Steel et al. 1984). Together with the seafloor spreading the western margin started to develop along the Senja Fracture Zone north till the southern limit of the Hornsund Fault Zone. Initially the margin had a continent-continent shear, which was followed by continent-ocean shear (Faleide et al. 2008, Smelror et al. 2009). By Late Eocene, the seafloor spreading had reached areas west of Spitsbergen (Faleide et al. 2008). Following the termination of spreading in the Labrador Sea, the spreading direction in the Norway-Greenland Sea was reorganised. The spreading changed from NNW-SSE to NW-SE, sometime between middle Eocene and Early Oligocene (Eidvin et al. 1998, Smelror et al. 2009, Czuba 2014).

3.1.4 Oligocene

From earliest Oligocene transtensional movement dominates the western margin along the DeGeer Zone (Ritzmann et al. 2003, Blinova et al. 2009). At this time the seafloor spreading is well established and the margin along he Senja Fracture Zone has become passive and formation of ocean crust starts (Faleide et al. 2008, Blinova et al. 2009).The oblique extension along western Spitsbergen lead to normal faulting, collapse of earlier compressional structures, down-faulting of blocks on the west side of Hornsund Fault Zone and the formation of the final graben geometry (Blinova et al. 2009). Towards the end of the Oligocene, seafloor spreading starts at the Knipovich Ridge. (Ritzmann et al. 2003, Czuba 2014). During this time the

Knølegga Fault and its associated fault system was reactivated (Eidvin et al. 1998), and there is a regional uplift (Grogan et al. 1999)

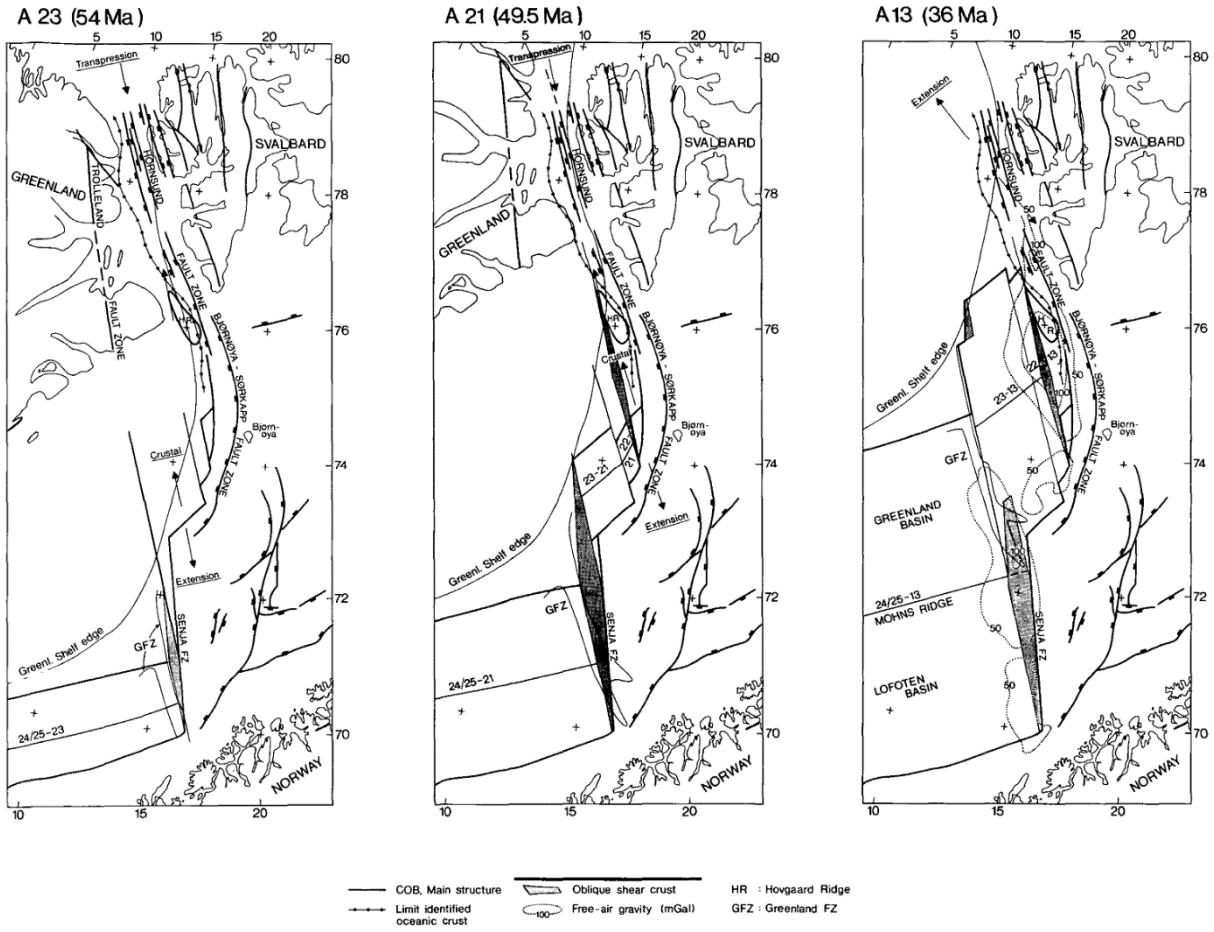

Figure 4: Pre-Oligocene plate reconstruction between Greenland and the western Barents Sea margin (Eldholm et al. 1987).

3.2 Sedimentological development

According to Anell et al. (2016) the youngest preserved sedimentary successions on the northwestern Barents Shelf are generally Late Triassic or Jurassic, and in places Early Cretaceous.

Following a Late Cretaceous transgression, the Paleocene to Oligocene deposits are a uniform sequence of outer sublittoral to deep-shelf claystone with minor siltstone, tuffaceous and carbonaceous horizons (Brekke et al. 2001). These form what we today call the Torsk Formation (Sættem et al. 1994). The Torsk Formation consists of generally light to medium grey or greenish grey claystone, which generally are non-calcareous (Dalland et al. 1988). The Paleocene succession found in the Sørvestnaget Basinis dominated by greyish mudrocks, followed by varicoloured red, grey, greenish and blackish mudrocks. These fine grained

depositions are interpreted to be from a low energy deep marine setting (Ryseth et al. 2003). The Paleogene analogue on Svalbard is the Central Basin. The Paleocene to Eocene succession found in the Central Basin on Svalbard are called the Van Mijenfjorden Group. The succession is between 1.5km and 2.5km tapering from southwest to northeast. The asymmetry towards the margin is implied to be caused by the tensional setting at the time (Steel et al. 1984). The Firkanten Formation is a part of the Van Mijenfjorden Gr. and represents the Paleocene succession. The formation can be further divided into two member, Todalen Mbr and Endalen Mbr (Steel et al. 1984, Livšic 1992). The Firkanten Fm seem to indicate an early shallower condition dominated by fluvial and tidal depositions (Todalen Mbr) going in to a more marine setting with wave-dominated sand sequences (Endalen-Kalthoffbergen Mbr) (Steel et al. 1984).

During the Paleocene-Eocene transition, it is believed that the sediment source area changed from northeast, east and southeast to west. Eocene successions indicate that during the time there were an increase in clastic deposition from Paleocene time, in western margin basins (Smelror et al. 2009). In the Central Basin, the start of the Eocene succession is represented by the Grumantbyen Formation. The formation indicates shallow marine environments, with deposition of fossiliferous sandstones (contains fossils) (Steel et al. 1984, Livšic 1992). Following the Grumantbyen Fm, there is the Hollendardalen Formation, which by many is considered a part of the Gilsonryggen Formation (Livšic 1992). The Hollendardalen Fm contains mudstones, siltstones and sandstones with coal seams, containing fossils and plant remains, and is restricted to the southeastern part of the Central Basin (Livšic 1992). The overlaying Gilsonryggen Formation is a wedge of tidal-influenced deltaic deposits at the base, followed by black shales and occasional siltstones. The formation rests on the erosion surface of the Hollendardalen Fm in the southeast and on the Grumantbyen Fm in the rest of the basin (Steel et al. 1984, Livšic 1992). Battfjellet Formation signifies the end of the Eocene succession. The depositional environment of the formation is interpreted to be wave-dominated delta, representing a prograding coastline. The succession is upwards coarsening and the sediment thickness generally increase from northeast to southwest (Steel et al. 1984, Livšic 1992). In the Sørvestnaget Basin the Eocene depositional environment is interpreted to be a continental shelf setting, where deposition happen through suspension deposition and are deposited beneath storm wave base (Sættem et al. 1994).

The Cenozoic succession of the Western Barents Shelf stems from several events of extensive erosion and redeposition (Eidvin et al. 1998). The extent of the uplift and erosion is a widely discussed subject and several models have been proposed. Figure 5 shows a model from

Henriksen et al. (2011) where he proposes a range of Cenozoic erosion from 0m to >3000m. Along the western margin the Harstad, Tromsø, and Sørvestnaget Basins, Vestbakken Volcanic Province and the areas west for the Knølegga Fault and Hornsund Fault Complex were principle areas of clastic deposition (Smelror et al. 2009).

The change to glacial deposition during the Northern Hemisphere Glaciation 2.6Ma ago can be seen as a distinct unconformity over the entire shelf. The unconformity changes to a downlap surface for prograding wedges of sandy and silty muds on the slope. These wedges derive the sediments from the mainland. On the Barents Shelf Plio-Pleistocene, uplift and glacial erosion led to deposition of large submarine fans along the margin, causing a regional tilt of the margin. These glacial deposits make-up over half the post-opening sediments of the Barents Sea (Faleide et al. 2008).

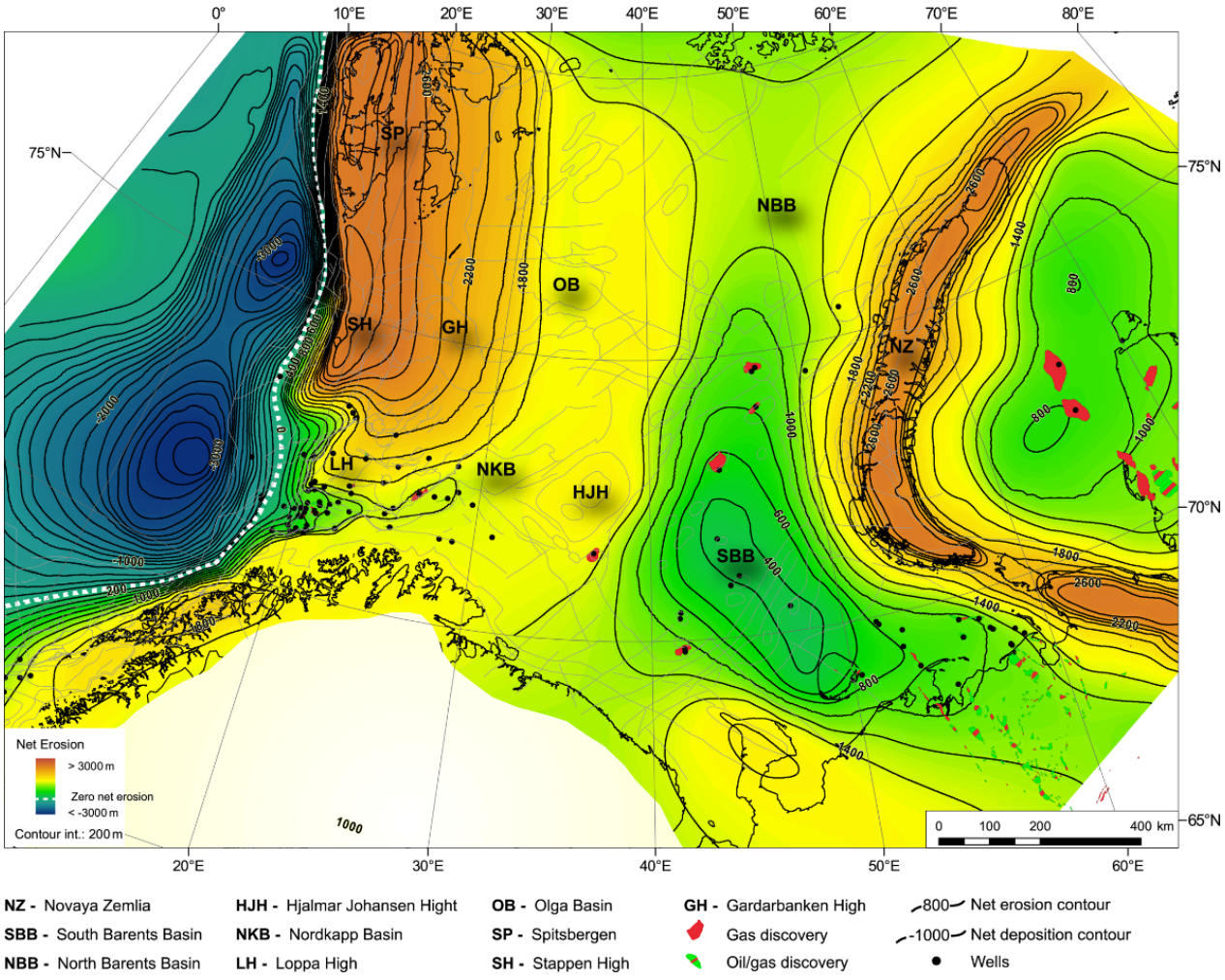

Figure 5: The estimated net erosion for the Barents Shelf (Henriksen et al. 2011)

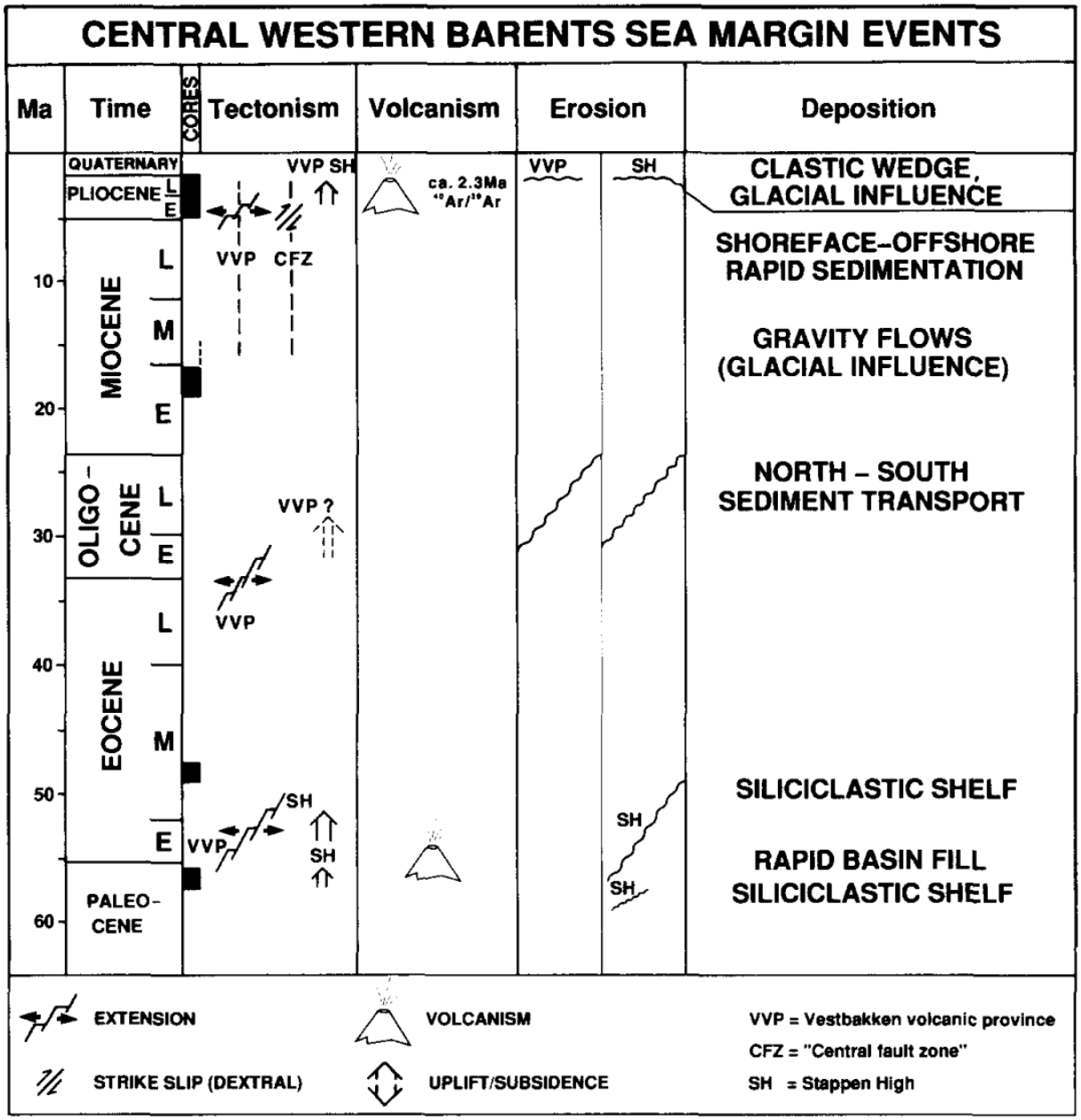

Figure 6: Margin events for the central western Barents Sea. (Sættem et al. 1994)

4 Material and Methods

4.1 Shallow cores and stratigraphic logging

General information

Wellbore name	7418/1-U-1	7517/12-U-1
Type	OTHER	OTHER
Purpose	SCIENTIFIC	SCIENTIFIC
Well name	7418/1-U-1	7517/12-U-1
Drilling operator	IKU Petroleumsforskning SINTEF Gruppen	IKU Petroleumsforskning SINTEF Gruppen
Drilled in production licence		
Entered date	23.08.1994	29.07.1994
Completed date	28.08.1994	04.08.1994
Drill permit	313-G	314-G
Kelly bushing elevation [m]	0.0	0.0
Total depth (MD) [mRKB]	311.0	359.0
Water depth [m]	182.0	156.0
Main area	UNOPENEDAREA	UNOPENEDAREA
Drilling facility		
Geodetic datum	ED50	ED50
NS degrees	74° 52' 33.3 '' N	75° 14' 16.4 '' N
EW degrees	18° 5' 48.8 '' E	17° 44' 59.2 '' E
NS UTM [m]	8312348.94	8352199.63
EW UTM [m]	590159.90	578189.18
UTM zone	33	33
NPDID wellbore	2185	2186

Table 1: Official information given by the NPD at their fact page. (NPD 2017)

The cores analysed in this thesis are a part of the Norwegian Petroleum Directorates Barents Sea-north mapping program. The cores where acquired by SINTEF, Stiftelsen for Industriell og Teknisk Forskning (Foundation for industrial and technical research), formerly the Institutt for Kontinentalsokkelundersøkelser (Institute for continental shelf investigations), IKU, on behalf of NPD. The cores where drilled northwest of Bjørnøya at 74°52'33.3"N, 18°5'48.8"E, 7418/1-U-1, and 75°14'16.4"N, 17°44'59.2"E, 7517/12-U-1.

Shallow cores are a classification given to boreholes that do not penetrate deeper than 560m below the seabed (Rise et al. 1994). The main objective of these kinds of investigations are to acquire geological information on the strata subcropping within a few hundred meters of the seabed. This includes stratigraphic control, source rock potential and reservoir and cap rock properties. At times, they can also be used for more specific objectives (Bugge et al. 1995). The boreholes have been routinely logged since 1987 with gamma, sonic, density, neutron porosity, dip/micro-resistivity and caliper logs (Rise et al. 1994, Bugge et al. 1995). Because they are shallow boreholes, it becomes necessary to take advantage of dipping strata in order to access older lithology.

The coring technique used for shallow boreholes are a combination of the offshore drilling technique and a slimhole diamond coring machine The diamond-coring machine rides in a piggyback position on the outer drill-string. The piggyback position is when the diamond-coring machine is placed on top of the heave compensated, non-rotating outer drill-string. The placement of the diamond-coring machine can be seen in

Figure 7. With this set up the diamond-coring machine can take advantage of the heave compensation of the outer drill-string to operate as if on land (Rise 1994). The diamond coring method gives a 54.5mm diameter core in segments of 3.05m (Rise et al. 1994, Bugge et al. 1995). The recovery time for this process is slowed down by winching time but mainly affected by the bedrock conditions. Average rate is about 2m/hr, provided no problems are encountered (Rise et al. 1994). The technique gives a high recovery rate with an average of 93%, but a large portion of the rocks in the cores have been poorly consolidated and fractured (Rise et al. 1994).

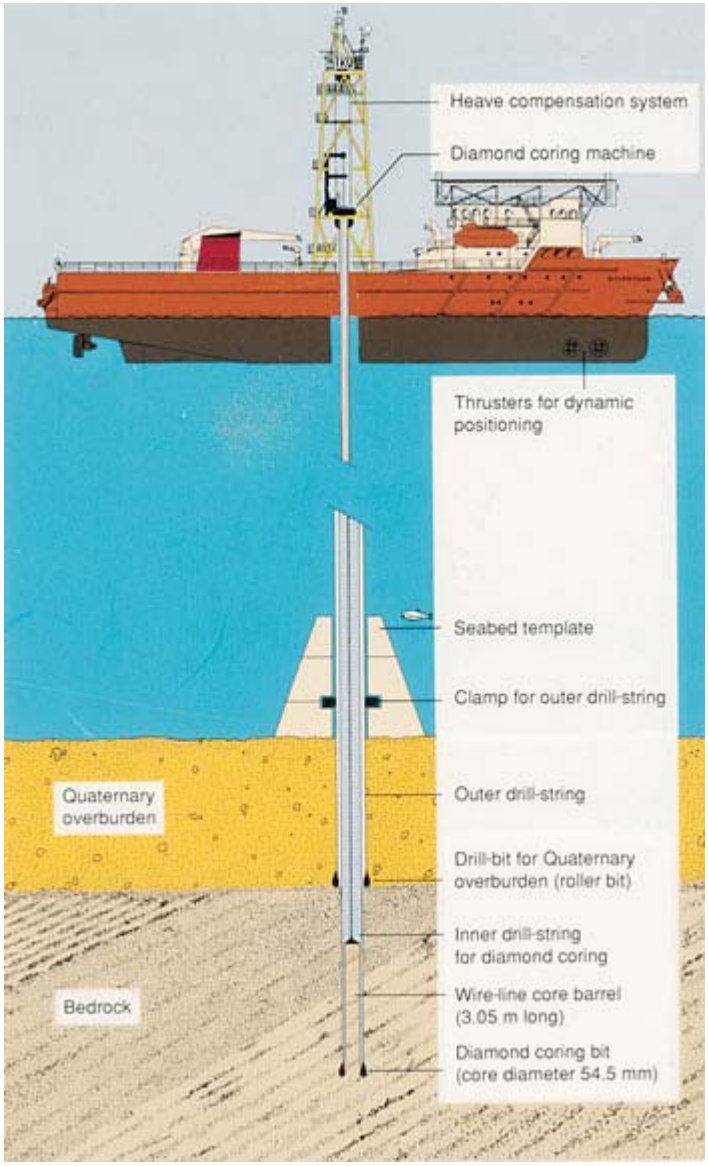

Figure 7: Diagram showing the configuration used during shallow stratigraphic drilling (2008).

The shallow drilling technique has been developed by IKU since 1975 when it was first tested in the shallow waters outside of Shetland. It has since been modified several times to the technique that is used today (Rise et al. 1994). The majority of the shallow cores were drilled using the Norwegian drillship M/S Bucentaur, which is specially design for geotechnical soil investigations. The ships drill winch is a limiting factor in the depth range of the drilling operation. The current range is about 700m-1000m below sea level. The use of floaters, alternative string material and smaller diameter drill bits have been proposed to extend the range further (Rise et al. 1994). Taking advantage of the dipping strata to core older successions make the shallow cores a cost effective alternative to deep exploration wells. The shallow cores have therefore become the main geological database for the northern Barents Sea (Riis et al. 2008).

After the cores are extracted, they are cut into several sections according to the diagram shown in

Figure 8.

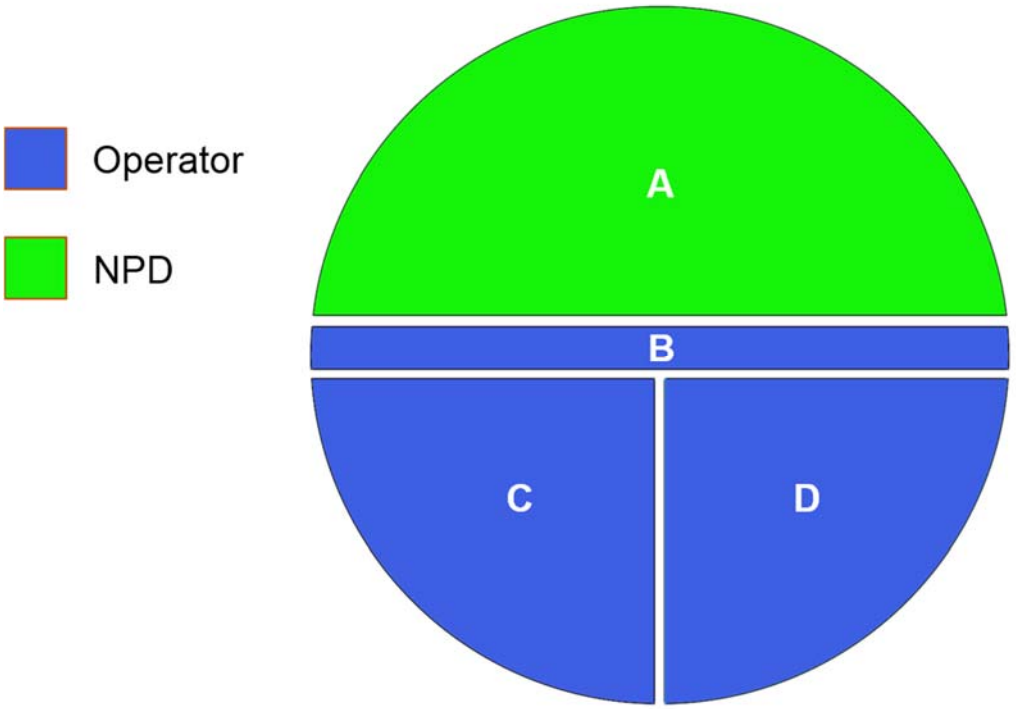

Figure 8: Diagram showing the sections cores are divided into after retrieval. NPD (internal)

The cores have been investigated over a three-day period at the Norwegian Petroleum Directorates core storage in Stavanger. Each core was laid out for viewing in boxes of four units of one meter each. For the investigation hand lenses, hydrochloric acid, grain size charts

Figure 9 and colour charts

Figure 10 were used. The cores were logged starting from the lower parts of the core going upwards, noting grain size, sedimentary structures, fossils, colour and any details of note. The results of the investigation were copied onto a geological core description diagram, which have later been reworked. The core logs can be seen in chapter 3 in Figure 6 and Figure 7. During the investigation, several photos were also taken for further reference.

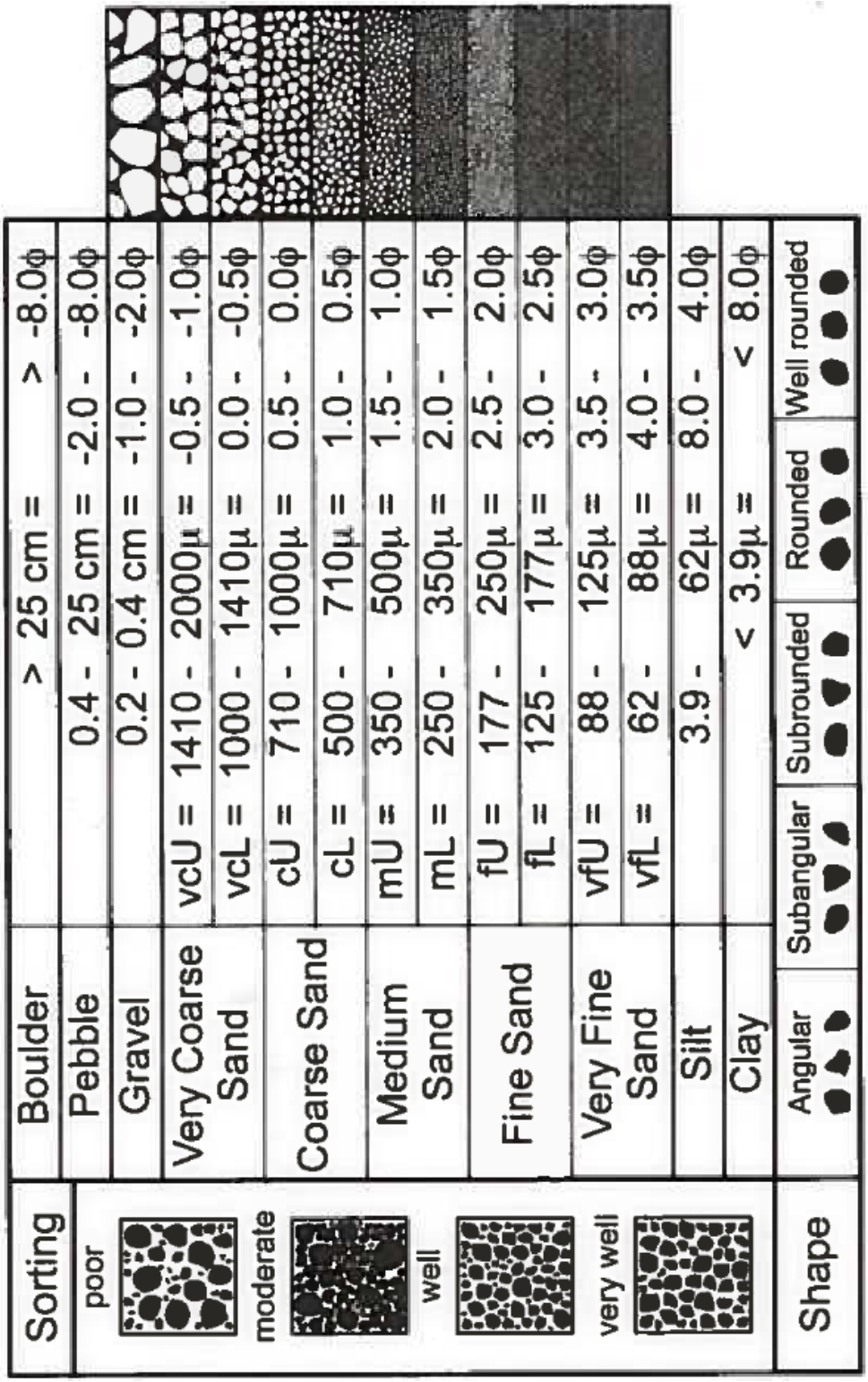

Figure 9: Grain size diagram with grain size, sorting and rounding qualifiers.

Figure 10: Munsell colour chart. Obs! Colours may appear differently depending on the medium it is presented on.

The advantage of using shallow cores for geological investigations is also the disadvantage and limiting factor. The scale of the data gives the best resolution one can get, but alone they lack the overview. When observing only a small portion the larger picture might be obscured (Figure 11). Cores are therefore frequently correlated with other cores and seismic to get a broader sense of the situation.

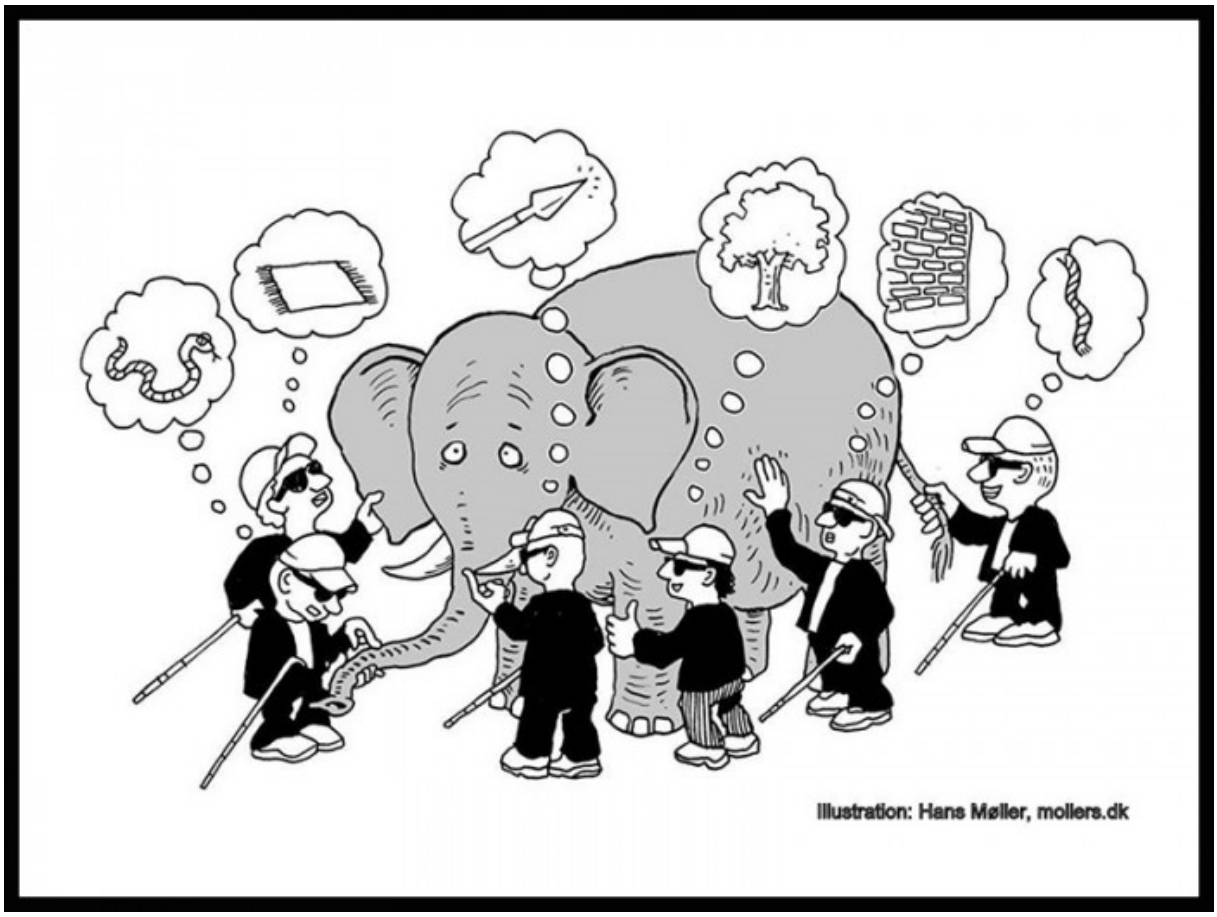

Figure 11: Illustration of the Indian fairy tale "the six blind men and the elephant". The story illustrates how a narrow focus can obscure the larger picture. Original drawing by Hans Møller. (Ayogo blog-patient engagement, 2015)

4.1.1 Sedimentology

A logical progression for the interpretation of sedimentary formations is presented in Figure 12.

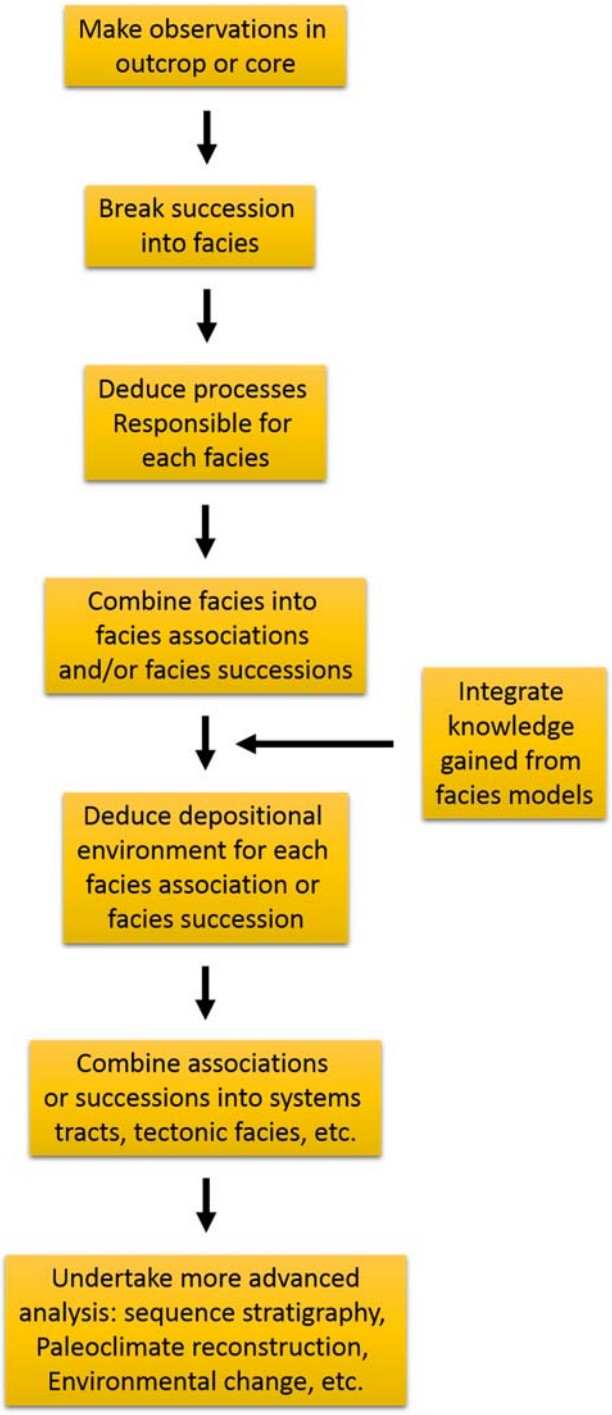

Figure 12: flow chart illustrating the work progression for determining a depositional environment. (Dalrymple, 2010)

By following a set procedure every time, one reduces the chances for error and make it easier to follow the interpretation process. The first step in the procedure is to make observations and describe your findings. Valuable observations for sedimentary rocks are grain size, sedimentary structures, other features (e.g. bioturbation, fossils etc.), thickness and boundaries.

4.1.1.1 Grain size

Grain size refers to the size of individual grains in sedimentary rocks. Grain size description uses a table (Figure 9) where grains are divided into groups dependent on size. This analysis is important as the size of grains is an important factor in their behaviour. During transport, larger sized grains settle faster than smaller sized grains. This effect can lead to sorting of grains, where you in some areas only find grains of a certain size. The relationship between the acting energy and the transport of loose grains is expressed in Figure 13. This diagram is called a Hjülstrom diagram. Reading the diagram shows that higher amounts of flow speed is needed to move cobbles than silt. This specific diagram shows the relationship for water at a depth of one meter. For other depths and mediums the relationship is different but the general trend is the same (Nichols 2009)

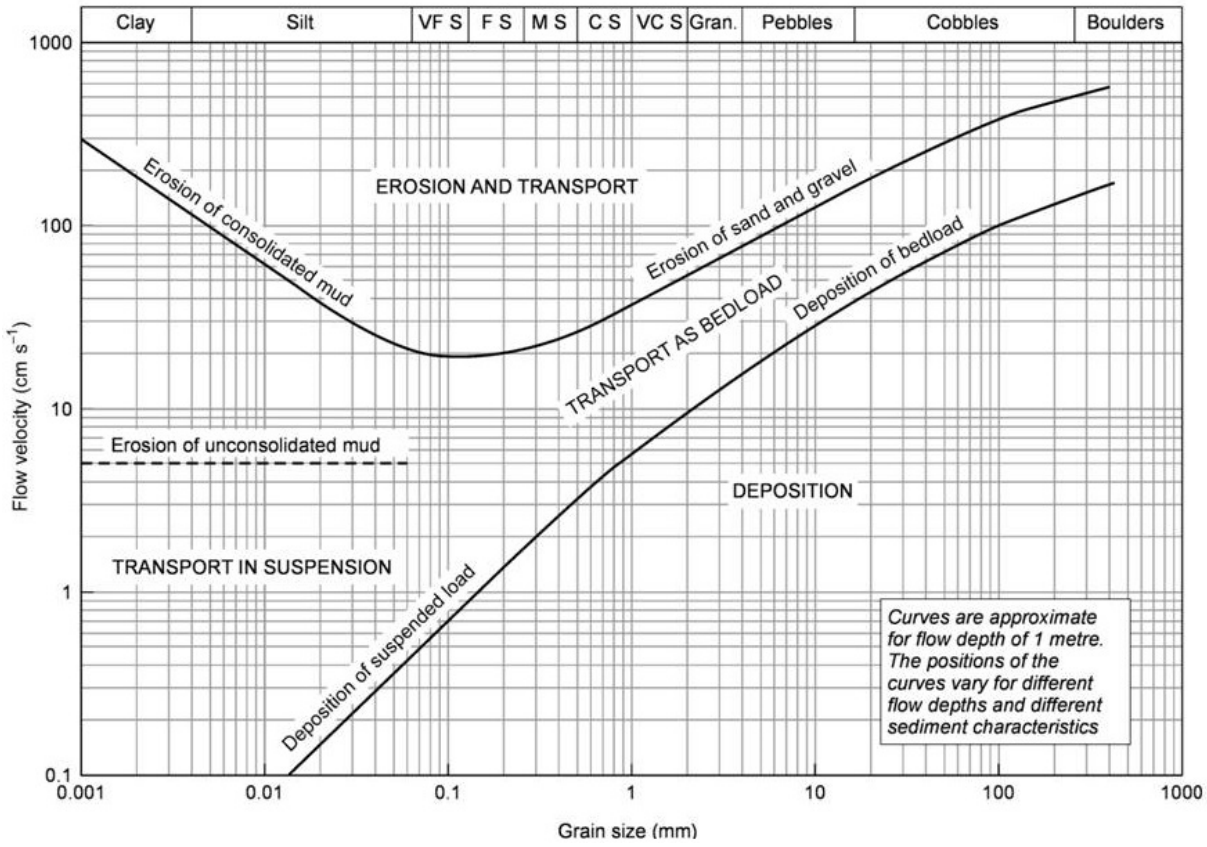

Figure 13: Hjülstrom diagram showing the relationship between flow velocity and loose grain transportation. Modified from Nichols (2009).

4.1.1.2 Sedimentary structures

During deposition of sediments, several factors contribute to the manner the sediments are arranged. The arrangement of sediments at deposition is called primary sedimentary structures. Primary sedimentary structures include, cross-bedding, wave ripples and horizontal lamination (Nichols 2009). The primary structures can be linked to the hydraulic energy during the environment, and a relationship between the energy, sediment size and structures can be expressed in a bedform stability diagram (Figure 14)

After deposition, any deformation of the sediments are referred to as post-depositional structures. Post-depositional structures are disruptive to the sediments and can often make it difficult to identify primary structures. The deformation of sediments can occur at any time after deposition up until lithification, and often involves density differences between

sedimentary layers (Nichols 2009).

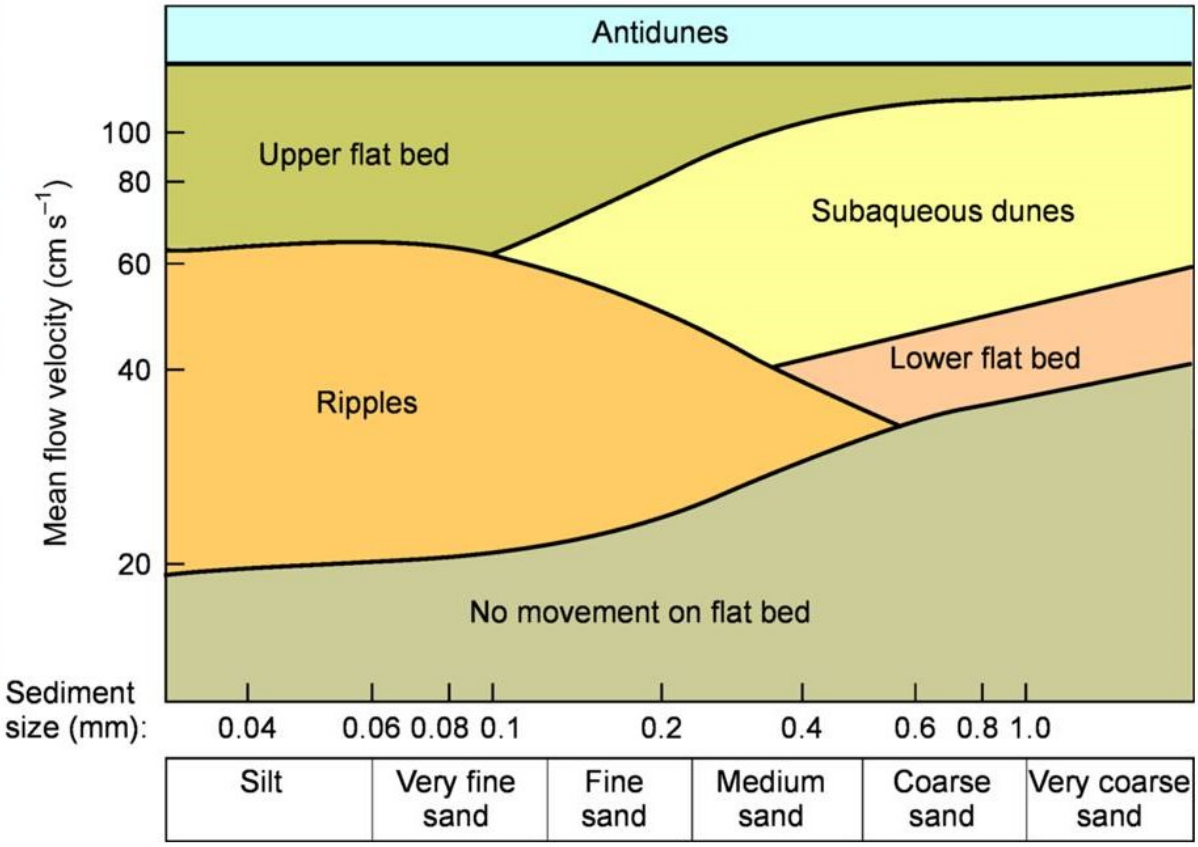

Figure 14: Bedform stability diagram. Shows the relationship between hydraulic energy, sediment size and primary sedimentary structures.(Nichols 2009)

4.1.1.3 Marine Environments

The marine setting is usually divided into several different environments based on the relative sea level. This is done to account for the impact sea level has on marine processes, like fair-weather eaves and storm waves. An idealized scenario is presented in

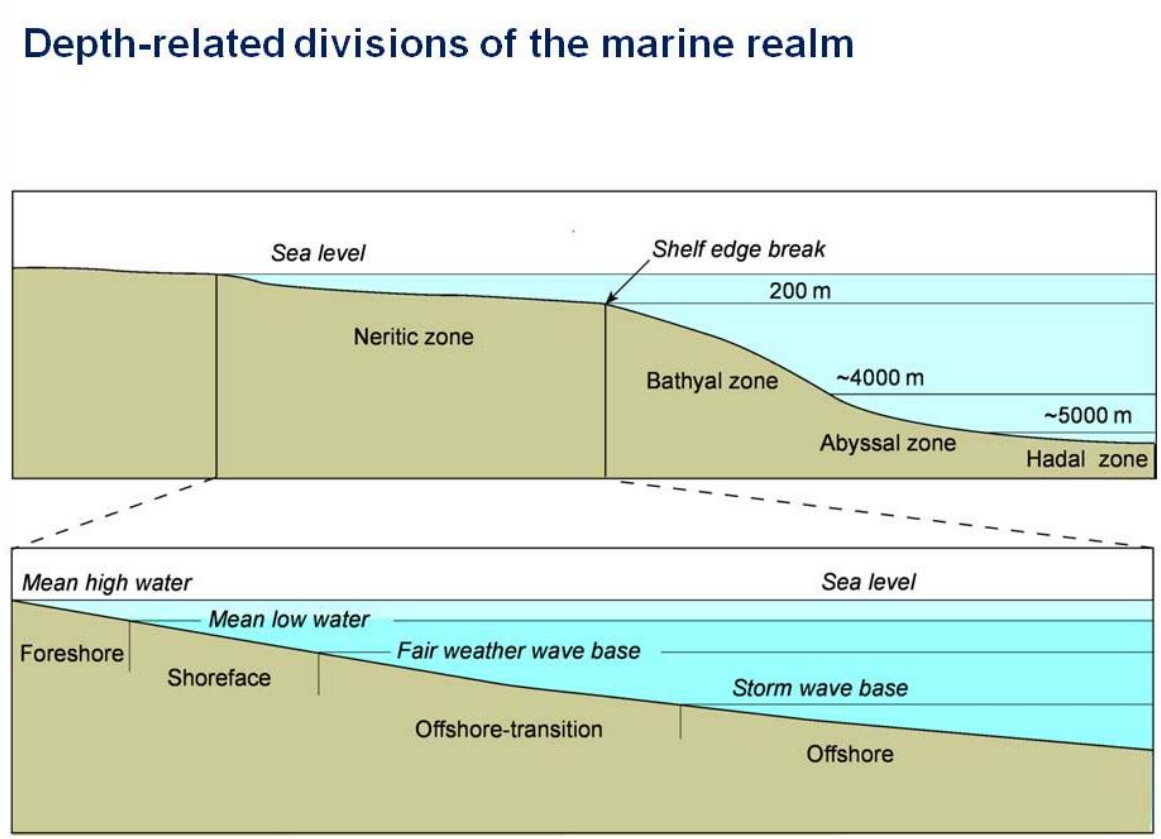

Figure 15: Division of the marine setting dependent on water depth.(Nichols 2009)

4.1.1.4 Ichnofacies

Ichnofacies is the description of trace fossils in a rock (Nichols 2009). Before the consolidation of sediments if the conditions are right macroscopic animals may set their marks on the sediments by moving on or in them. These marks can later be used to identify the organism which set the track, and this can in turn be used to postulate the environment during deposition as organisms are very sensitive to the environment (MacEachern et al. 2010). Some of the factors that influence the presence of these organisms are substrate consistency, food-resource type and distribution, energy conditions, salinity, oxygenation, water turbidity and deposition rate. These parameter are the controlling factors, and tend to change with water depth (Nichols 2009, MacEachern et al. 2010). Some assemblages of trace fossils can be indicative of water depth and a generalized scheme can be made Figure 16. The assemblages are named after certain characteristic ichnofauna, but these are not necessarily present, e.g. *Cruziana* facies does not necessarily contain actual *Cruziana* (MacEachern et al. 2010).

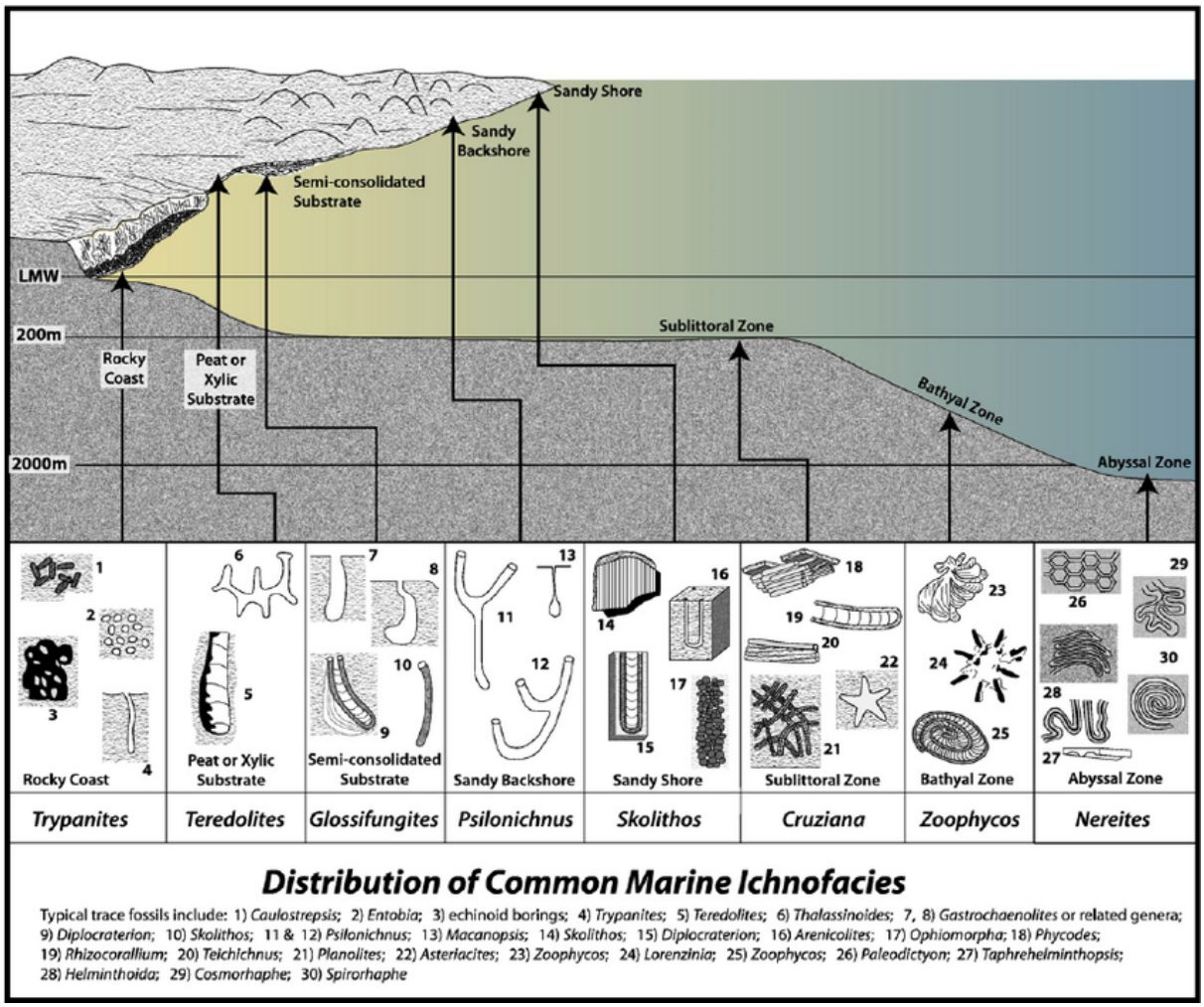

Figure 16: An idealized proximal-distal trend for icnofacies assemblages. (MacEachern et al. 2010)

Depending on the activity in the area the amount of bioturbation in a succession can vary from barely touched to several overlapping traces throughout the succession. The amount of bioturbation in a given sediment interval is graded accordingly (Nichols 2009, MacEachern et al. 2010):

Grade 1: A few discrete traces.
Grade 2: Bioturbation affects less than 30% of the sediments, bedding is distinct.
Grade 3: Between 30% and 60% of the sediments are affected, bedding is distinct.
Grade 4: 60% to 90% of the sediments are bioturbated, bedding is indistinct.
Grade 5: Over 90% of the sediments are bioturbated, bedding is barely detectable.
Grade 6: Sediments are totally reworked by bioturbation.

The amount of bioturbation from grade 1 to grade 5 is illustrated in Figure 17

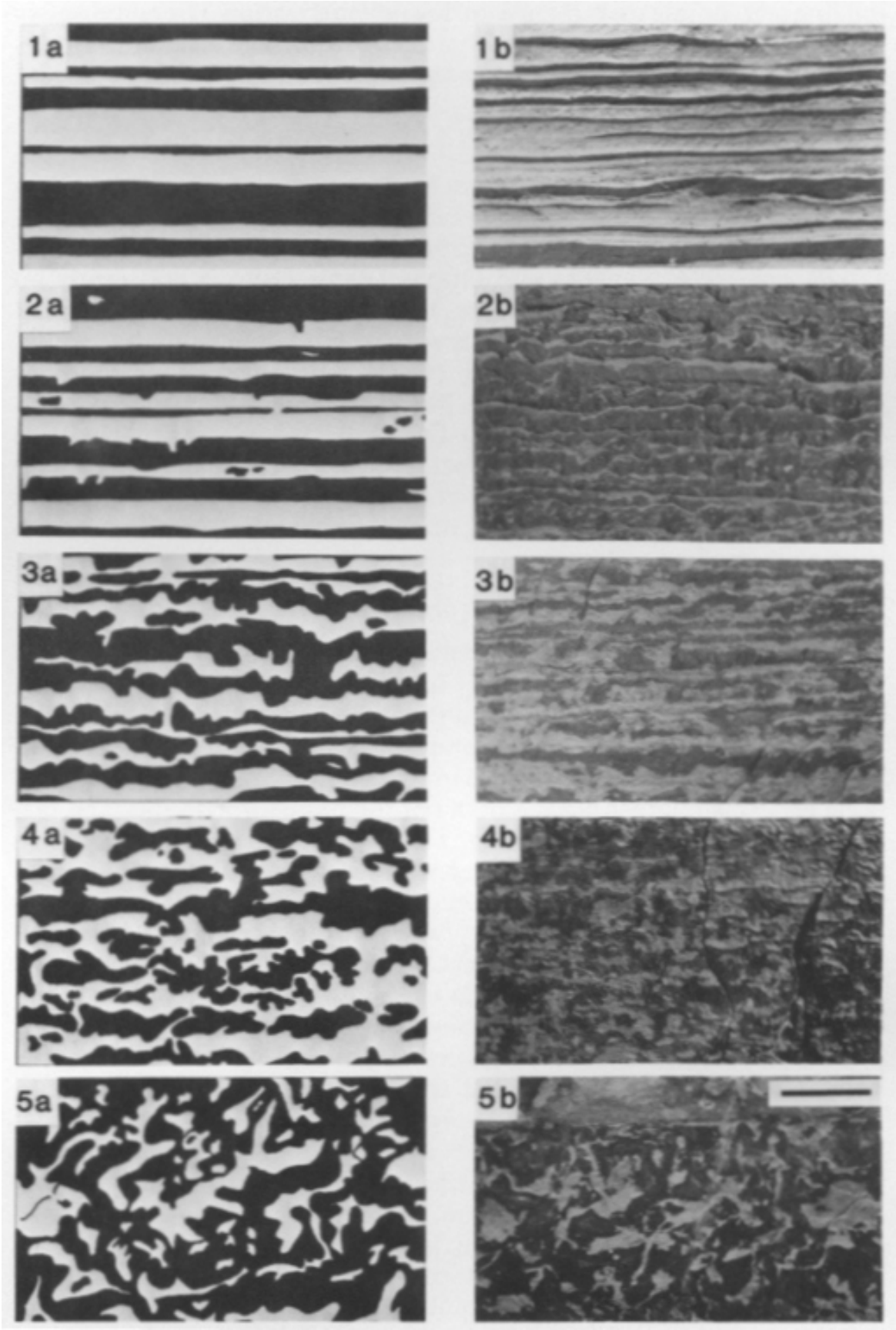

Figure 17: Bioturbation intensity chart with multiple examples of each grade from 1 to 5. From Droser et al. (1986)

Gingras et al. (2014) presented a flow chart useful for determining depositional environment based on the bioturbation of the deposits. Although a useful tool, it is important to remember than these methods are not sufficient alone and should be viewed in context with other methods to determine the most accurate interpretation possible.

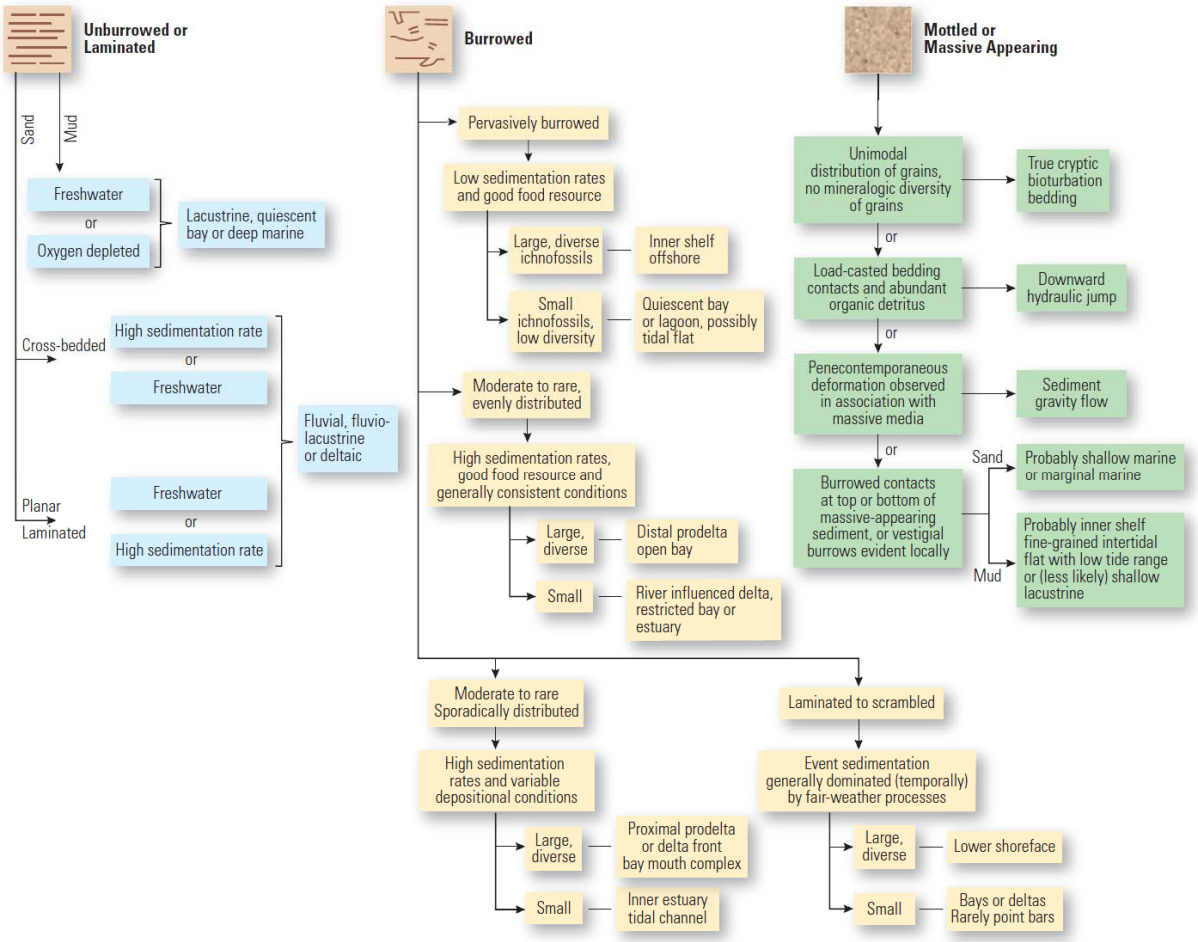

Figure 18: Flow chart for determining depositional environment based on the bioturbation of the formation. (Gingras et al. 2014)

4.1.2 Field equivalent

Because of the location of the boreholes, it is not possible to do outcrop investigations. However, parts of the Barents Sea Shelf are aerially exposed. The Svalbard Archipelago covers an area of 63 000km^2 which gives a comprehensive overview of the geology of the entire region (Worsley 2008). The Central Basin in Svalbard exposes Paleocene to Eocene succession, and comparing the findings in this study to other work from this area will be valuable to gather an understanding of the regional geology (Steel et al. 1984).

4.2 Methods of exploration, and scale

For any successful business, cost efficiency is key to prosperity. To avoid drilling expensive dry wells everywhere, oil companies apply a wide array of techniques to reduce the risk of drilling. These techniques are useful to understand the geology of the area and make an informed decision when it comes to whether to drill or not. These techniques range in scale and price, and the trend is that the smaller the scale the higher the price. Comparatively, borehole cores are the best resolution of the surveys applied in petroleum exploration, but also the most expensive (Figure 19). Therefore, other techniques are usually applied before drilling for cores.

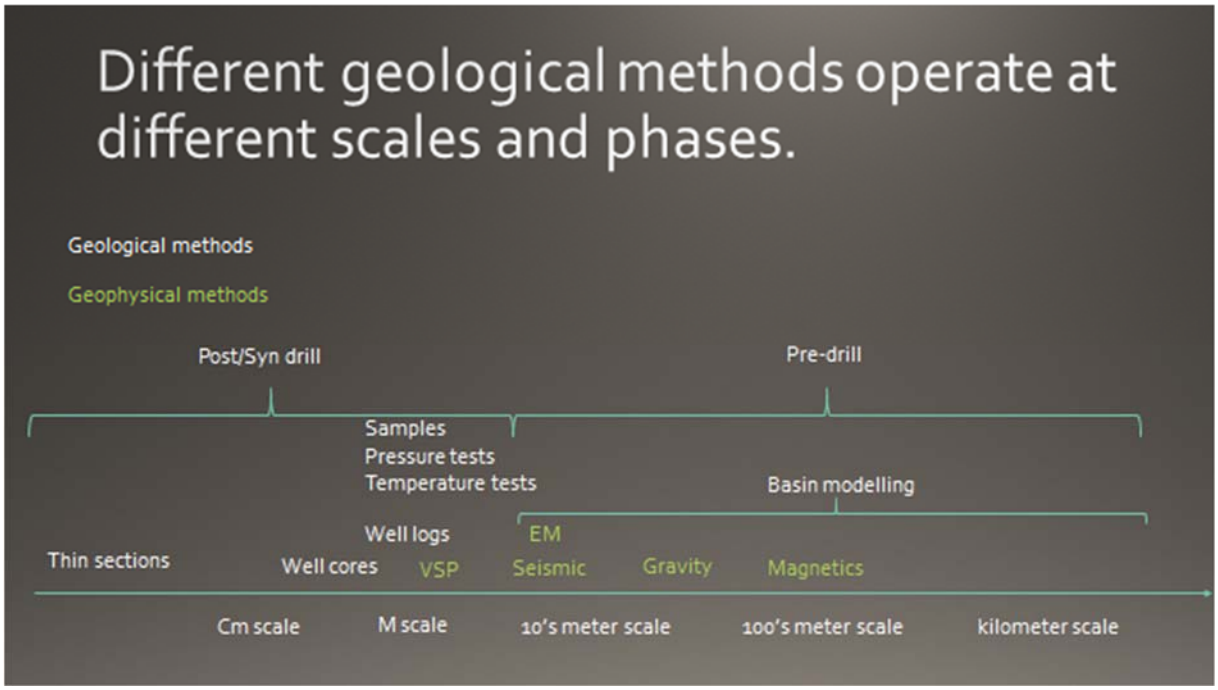

Figure 19: Diagram showing the scale and application of different exploration methods. (Martens 2016)

When comparing the different methods of exploration, the scale or resolution of the method is important to consider. The largest scale investigations are the magnetic and gravimetric surveys. These surveys are usually large-scale surveys covering great areas. The resolution therefore tends to be lower and few details can be mapped. The main use of these large-scale surveys are to identifying the scale and limits of sedimentary basins (Selley et al. 2015). Following large-scale investigations 2D-seismic surveys would be carried out. The resolution of 2D-seismic is much higher than gravimetric and magnetic surveys, but the cost is in return also higher. In seismic surveys, the resolution is dependent on the depth of investigation. The horizontal resolution can be calculated by the formula:

$$r = \frac{v}{2}\sqrt{\frac{t}{f}} \quad (1)$$

r: radius v: velocity t: two-way travel time f: frequency

(Sheriff 1980)

The number given by the formula is the radius of a circle, called the Fresnel zone. The horizontal resolution can be improved by migrating the seismic data. This process collapses the Fresnel zone and gives a much higher resolution, which can be calculated by the formula:

$$r = \frac{\lambda}{4} \quad (2)$$

r: radius λ: wavelength

(Brown 1999)

In 2D-seismic the Fresnel zone can only be collapsed in the inline direction, and so the horizontal resolution in the crossline direction is still calculated according to the formula.

Following 2D-seismic investigations, 3D-seismic surveys are generally carried out. 3d-seismic surveys work on the same principal as 2D-seismic, but are instead done in a grid fashion by using several receivers. This way the received signals can be compiled in to a 3D image. The nature of this way of collecting data makes it possible to collapse the Fresnel zone in both the inline and crossline direction, ultimately giving a higher resolution still (Brown 1999).

The investigations down to 3D-seismics are still done on a somewhat large scale, and used for mapping out possible prospects. Following this mapping process, wells can be bored to evaluate a prospect. During and after drilling there are several investigations that can be done. Most common and cheapest are the well logs. Well logs are a series of continuous investigations done either during or after drilling. The logs gathered span a range of different petrophysical properties, giving an insight into the properties and quality of the prospect. Common well logs are caliper, resistivity, gamma, neutron, density, sonic and dip logs. The resolution of these investigations vary with depth of investigation, but they are generally some tens of centimetres (Rider et al. 2011, Selley et al. 2015).

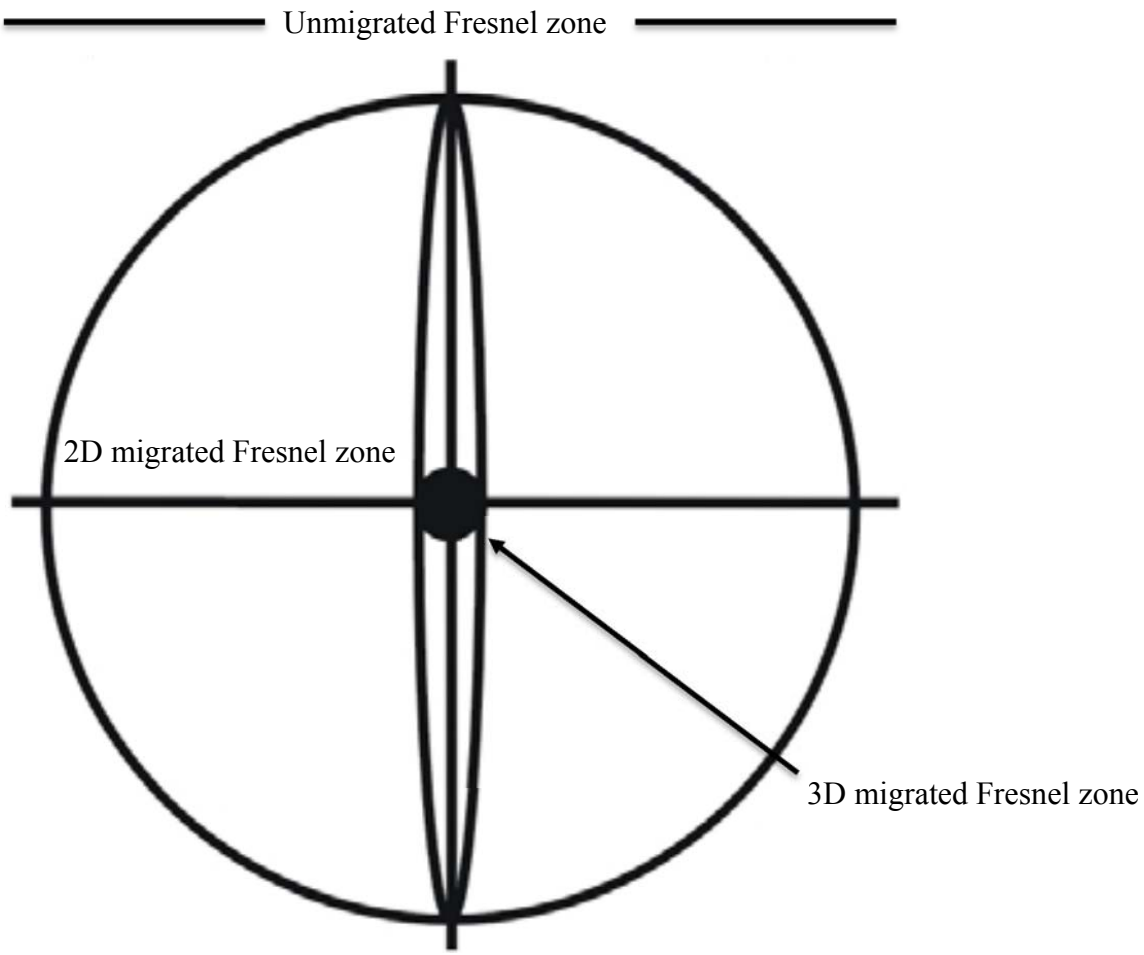

Figure 20: Diagram of the Fresnel zone, unmigrated, 2D migrated and 3D migrated. (Brown 1999)

The last type of investigation that can be done are well cores. Well cores can be extracted during drilling to get a direct sample from the formation that is being drilled. This is the highest resolution investigation that can be done, as it is an actual sample of the rocks that the other methods are trying to describe. The core itself can be described, and if further information is needed one can take samples from it to analyse.

5 Results

All depth measurements in this study is done relative to the drillship's Kelly Bushing. The elevation of the Kelly Bushing in both cases were 0.0m above sea level. The depths of the core are given in mRKB, but annotated as m for simplicity's sake.

5.1 7418/01-U-01

The borehole reaches a total depth of 311.0m, at a water depth of 182.0m. The penetrated quaternary overburden was 7.5m, and beneath that, 116.75m of sedimentary rocks were penetrated. Of the penetrated sedimentary rocks 95.5% was recovered in cores, making the total core length 113.0m.

5.1.1 Description

The grain size distribution of the core-log presents a pattern of three different sections that can be seen throughout the entire core length. The core can be divided into a bottom, middle and top section, henceforth referred to as Section A, Section B and Section C respectively. Each section is separated by a conglomerate (Figure 21).

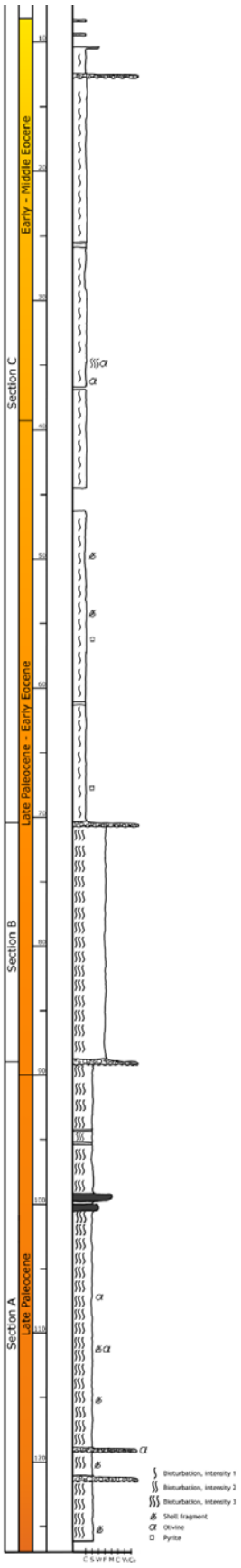

Figure 21: Stratigraphic log of core 7418/1-U-1

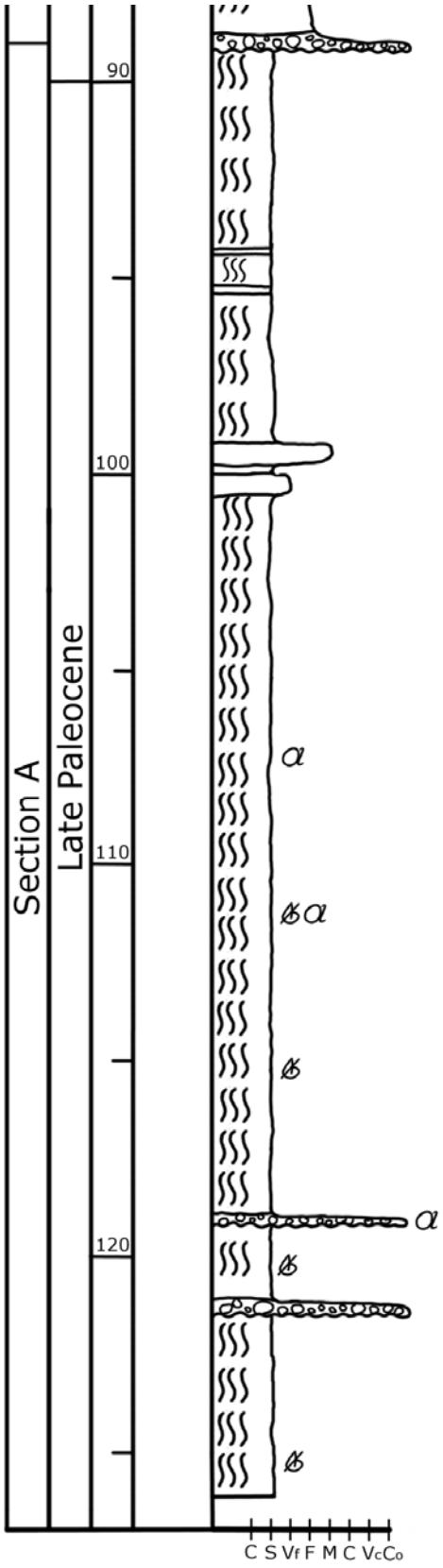

Figure 22: Crop of 7418/01-U-01 Section A

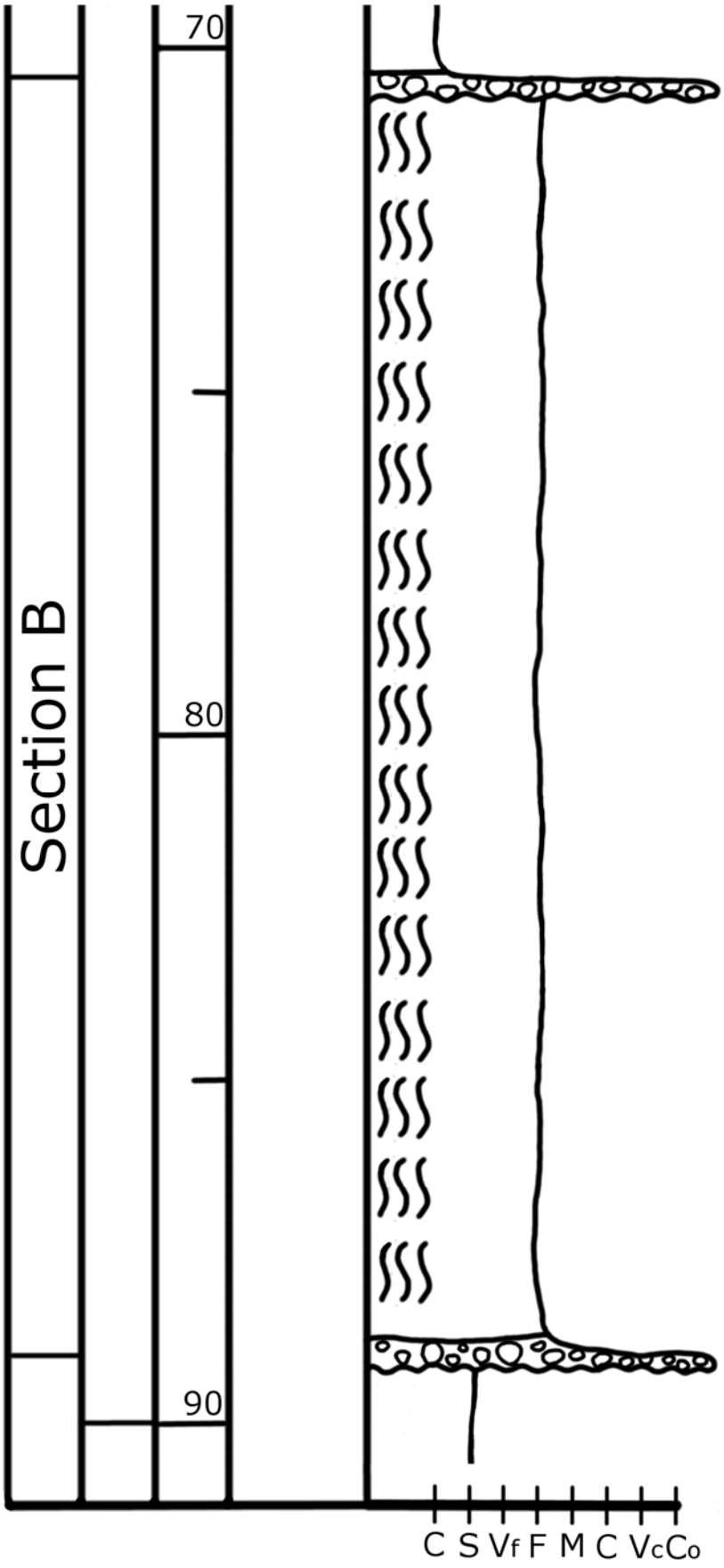

Figure 23: Crop of 7418/01-U-01 Section B

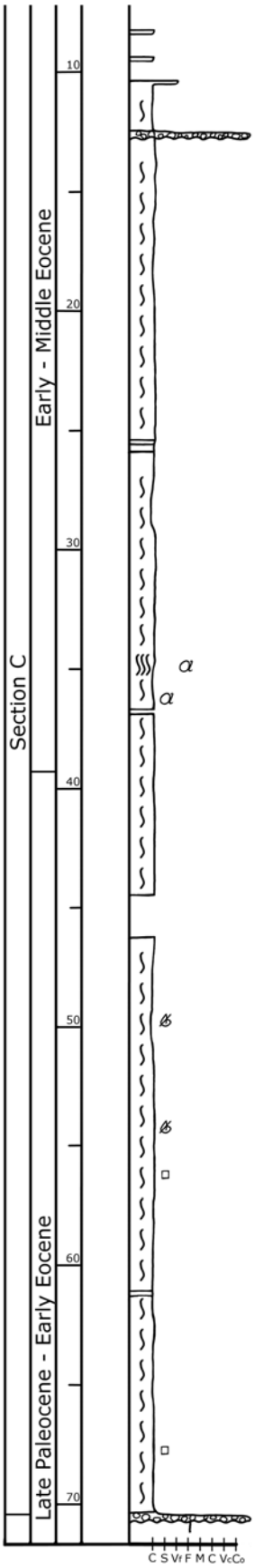

Figure 24: Crop of 7418/01-U-01 Section C

5.1.1.1 Section A 126.15m-89.2m

The bottom section starts at 126.15m and stretches to the third conglomerate at 89.2m. The section consists of mainly dark grey siltstones, with the occasional conglomerate and some dark fibrous intervals. The interval shows (weak) signs of primary sedimentary structures, indicating some darker laminations between the darker grey sediments. Most of the structures are however obscured, making it difficult to determine primary structures precisely. There are some shell fragments throughout the section with calcitic composition, as evident by their reaction to hydrochloric acid.

The conglomerates in this section are located at 121.2m, 119.2m and 89.2m. They are all matrix supported with vastly different composition.

The lowermost conglomerate at 121.2m is a polymictic matrix-supported conglomerate with sub-rounded (clasts) ranging from granule to cobble size, with a matrix of dark grey silty sediments.

The second conglomerate at 119.5m is a matrix-supported polymictic conglomerate. The clasts range from sub angular to sub rounded, with some angular green (olivine?) clasts, with a dark grey matrix of silty sediments. The green minerals differ from the rest of the clasts in the conglomerate in both size and roundness, suggesting different origins. The larger clasts seems to be concentrated in the lower parts of the conglomerate, suggesting a normal grading.

The upper conglomerate of this section is a polymictic clast-supported conglomerate. The clast size ranges from granules to cobbles with the larger clasts reaching sizes up to >20mm. The roundness of the clasts range from angular to well rounded, where the smaller size clasts a typically less rounded will the larger clasts show more rounding. The conglomerate shows inverse grading, with larger clast atop and smaller clasts on the erosional surface.

At 100m and 95m, there are shorter intervals with dark fibrous coarser grained deposits, standing out from the rest of the section. The orientation of these intervals seem to be in line with the depositional orientation of the rest of the section suggesting no angular unconformity.

Throughout the bottom section there are green mineral clasts occurring among the sediments at seemingly random intervals.

Figure 25: Conglomerate from core 7418/01-U-01 at 89.2m.

5.1.1.2 Section B 89.2-70.8m

The middle section starts after the conglomerate at 89.2m, described in the previous section, and stretches to a new conglomerate at 70.8m. The total length of the section is 18.4m. The entire section consists of fine sand dark grey in colour with lighter grey and darker grey to black laminations. The top conglomerate of this section is a matrix-supported polymictic conglomerate, with sub-rounded to rounded clasts. Clast size varies from pebble size down to sand size in the finer clasts. Some clasts of the green mineral seen previously in the core can be found in this conglomerate, varying greatly in size and shape/roundness. Some rust coloured intervals occur throughout this section, indicating the presence of iron bearing minerals in the sediments. Primary sedimentary structures are greatly (obscured), making determination of primary structures difficult. The lamination does however seem to be following the dipping trend of the previous section.

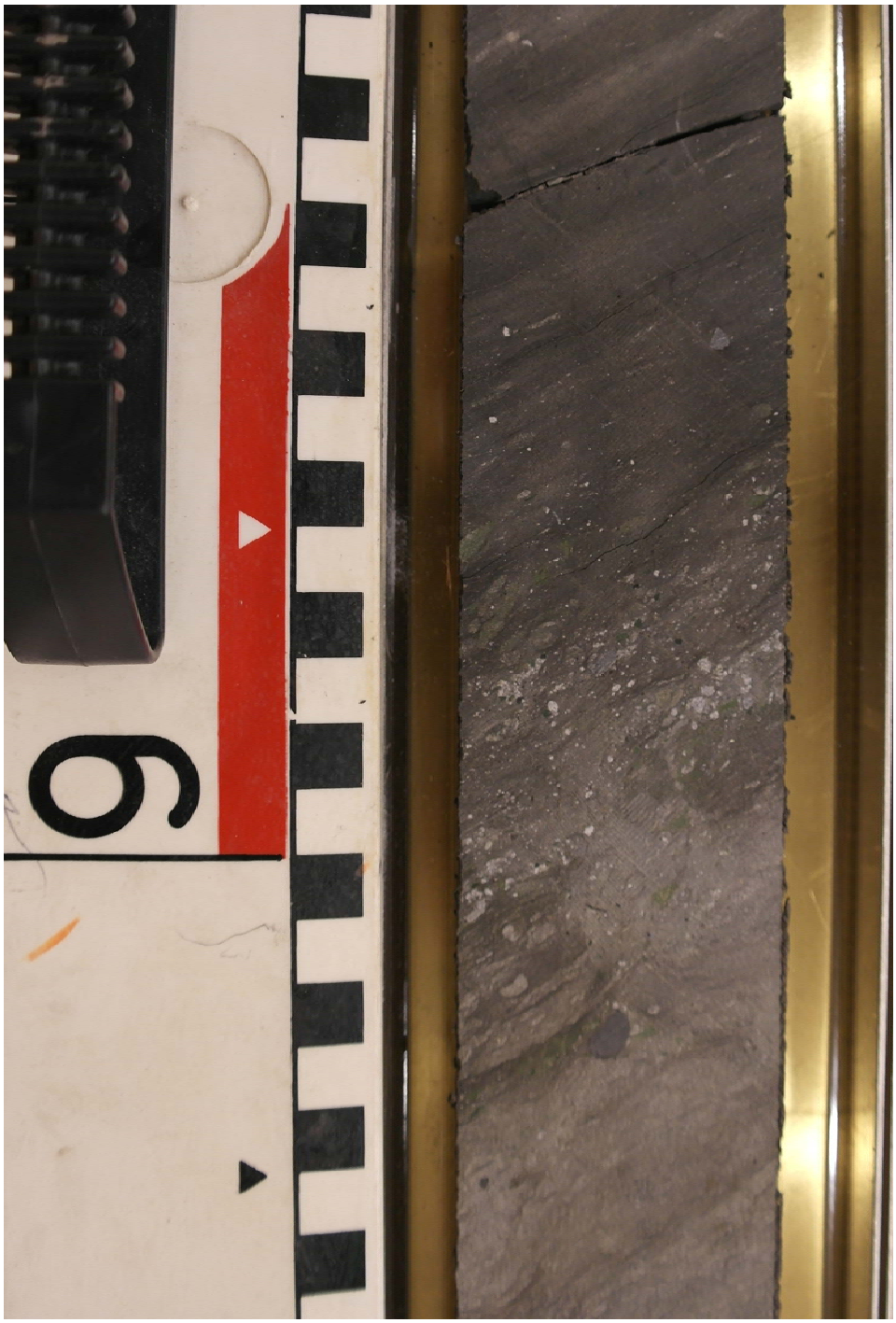

Figure 26: Conglomerate from core 7418/01-U-01 at 70.8m.

5.1.1.3 Section C 70.8m-8.4m

The top section starts at the terminating conglomerate of the middle section at 70.8m. The section consists of mainly mud-sized sediments with a small coarser interval towards the top end of the section. This section stretches to 8.4m although most of the upper 2.5m are missing. There are also some missing parts at 41m and 44.5m to 46.4m. The dominating lithology of this section is light bluish grey mudstone with dark grey coloured laminations. The boundaries

between the lighter and darker layers are indistinct throughout the section, but more so towards the top. Some colour variance also occur in the lighter layers changing between blue tinted greys to more green tinted browns.

Besides the lower conglomerate, that separates the middle and top section, the upper section has one conglomerate towards the top at 12.8m. The conglomerate is a matrix-supported polymictic (?) conglomerate with sub-angular to angular clasts. Clast size vary between pebbles and granules. At 60.2m, there is a 14cm interval of greyish orange coloured sediments showing no primary structures. Both upper and lower boundaries are sharp. At 25.9m, there is another coloured interval of 30cm. It is dark yellowish orange and moderate yellowish brown in colour, with sharp boundaries at both the start and termination of the layer (siderite?). Above the layer, there is a small interval of 9cm with fibrous dark grey rocks. The boundary atop of this fibrous interval is gradual back into the normal trend of the section. At the upper ten centimetres of this section, excluding the two separate sections at 9m and 8m, there is an abrupt change in coarseness from mud to fine sand. The boundary at this shift is obscured by fracturing of the core making it impossible to determine, although there is no evidence of grading so a sharp boundary is probable.

The upper section of this core contains the bulk of the green mineral that occurs throughout this core. This mineral occurs at 34.8m and 36.3m both times in without any distinct boundaries, suggesting no facies change. In both cases, there is large variance in clast size, and all clasts seem to be very angular in shape.

As in the previous section, there are several intervals that have a rust coloured tint to them indicating iron content in the sediments. There are also a clear rust coloured lamination at 67.2m, as well as a granule-sized nodule at 56.2m.

At 35.2m, there is a 20cm interval where the darker laminations are fibrous and flaky. The surrounding rocks are tinted in a very pale orange and moderate yellowish brown colour, or in a darker grey colour than the bulk of the section. The lower boundary seems to be gradual, but the top boundary seems to be sharp although the exact boundary is obstructed by a crack in the core.

5.1.2 Facies Description

5.1.2.1 Dark grey bioturbated siltstone

Section A of the core consists of mainly siltstones that have been heavily obscured by bioturbation to the point of making primary structures difficult to discern. The section show no change in grain size throughout, but is rather "cut" at the top by a conglomerate separating this from Section B. Within the section there is two conglomerates both of which are matrix-supported, as well as two sandy layers at 100m and 95m. The dominant bioturbation can be identified as *Phycosiphon*, *Scolicia*, *Skolithos*, *Chondrites*, *Planolithes* and *Schaubcylindrihnus* (NPD unpublished).

By the domination of siltstone in the section a low energy can be assumed from consulting a Hjülstrom diagram (Figure 13). Although the particular diagram shown in Figure 13 is for depths of one meter, the general trend of finer grained material settle in lower energy environments can be observed. From just observing the intensity of bioturbation we can assume that the depositional environment was suitable for life to thrive. Two main factors contribute to this, adequate food supply and low sedimentation rates (Gingras et al. 2014).

5.1.2.2 Dark grey bioturbated sandstone

Section B of this core comprises mainly fine grained sandstones that are intensely obscured by bioturbation. In this section, the primary structures of the formation was mostly no longer visible due to reworking caused by bioturbation. The bioturbation in this section is identified as *Planolites*, *Chondrites*, *Rosselia*, *Teichichnus*, *Schaubcylindrichnus*, *Phycosiphon*, bivalve burrows, *Palaeophycus* and *Scolithos* (NPD unpublished). The section starts at the conglomerate that separates this section from Section A. The conglomerate lays on an erosional surface indicating a mass movement.

The fine-grained sandstones indicate that although the depositional environment was low energy, it still was higher energy than during the deposition of Section A (Figure 13). As in Section A, the section is heavily bioturbated indicating low sedimentation rates.

5.1.2.3 Light bluish grey claystone

Section C of this core is dominated by claystone. Unlike the other two sections of this core, this section is not obscured by bioturbation. The section is horizontally laminated, with a gradual border between most lamina.

The lack of bioturbation indicates inhospitable conditions for fauna during deposition. This could stem from high sedimentation rates, low supply of food or anoxic conditions.

5.2 7517/12-U-01

The total drilled depth was 200.0m at a water depth of 156.0m. 110.7m of Quaternary overburden was penetrated before drilling 89.3m into the sedimentary rocks. The drilling gave a 98% recovery rate making the total length of the core 87.8m.

5.2.1 Description

The core is divided into six sections, A-F, based on grain size.

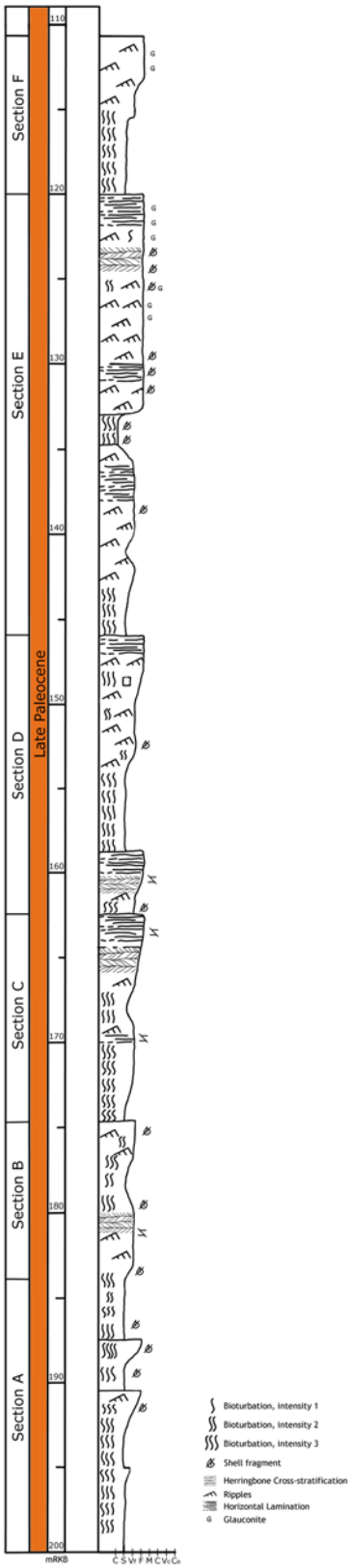

Figure 27: Stratigraphic log of core 7517/12-U-1

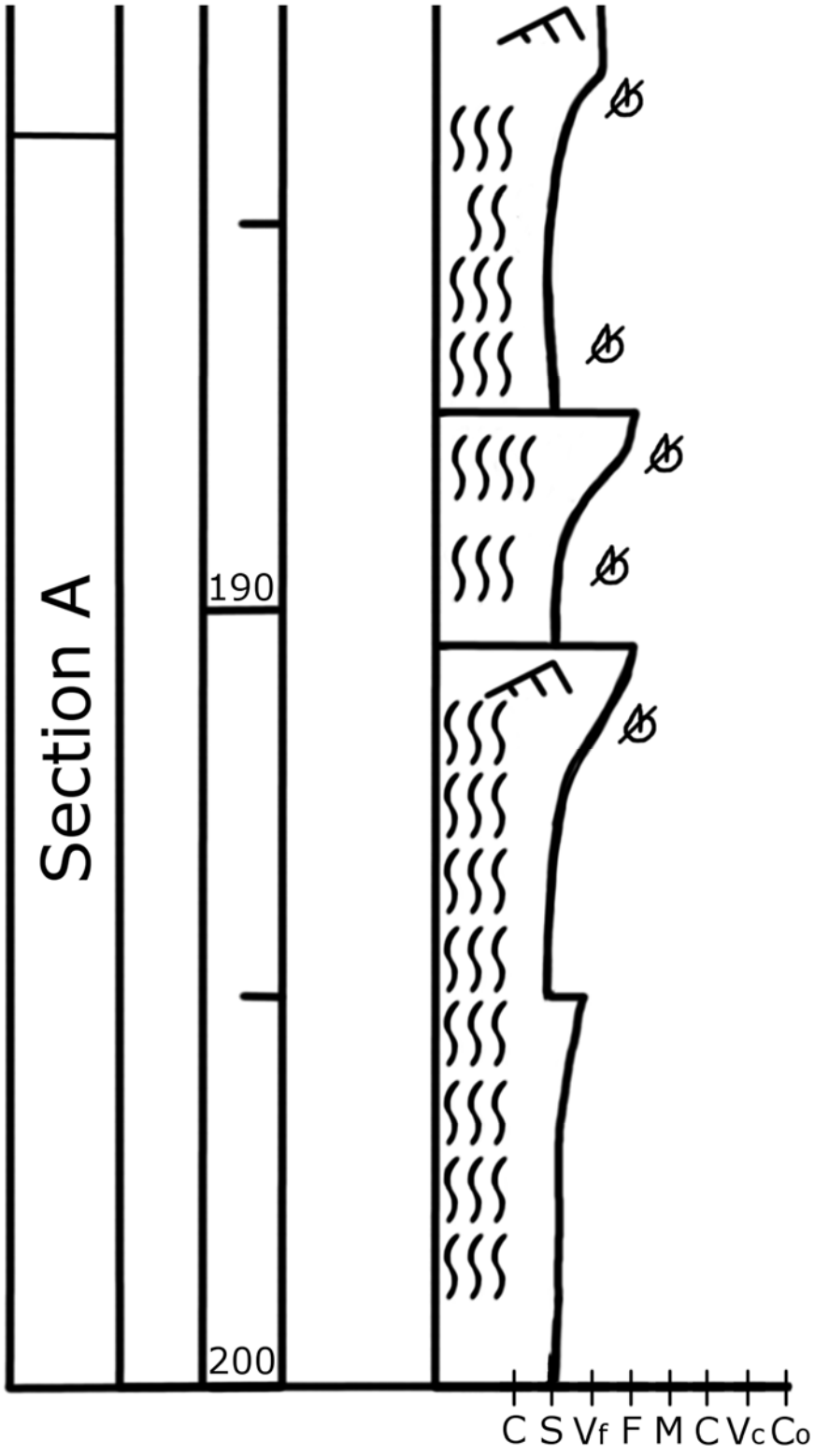

Figure 28: Crop of 7517/12-U-01 Section A

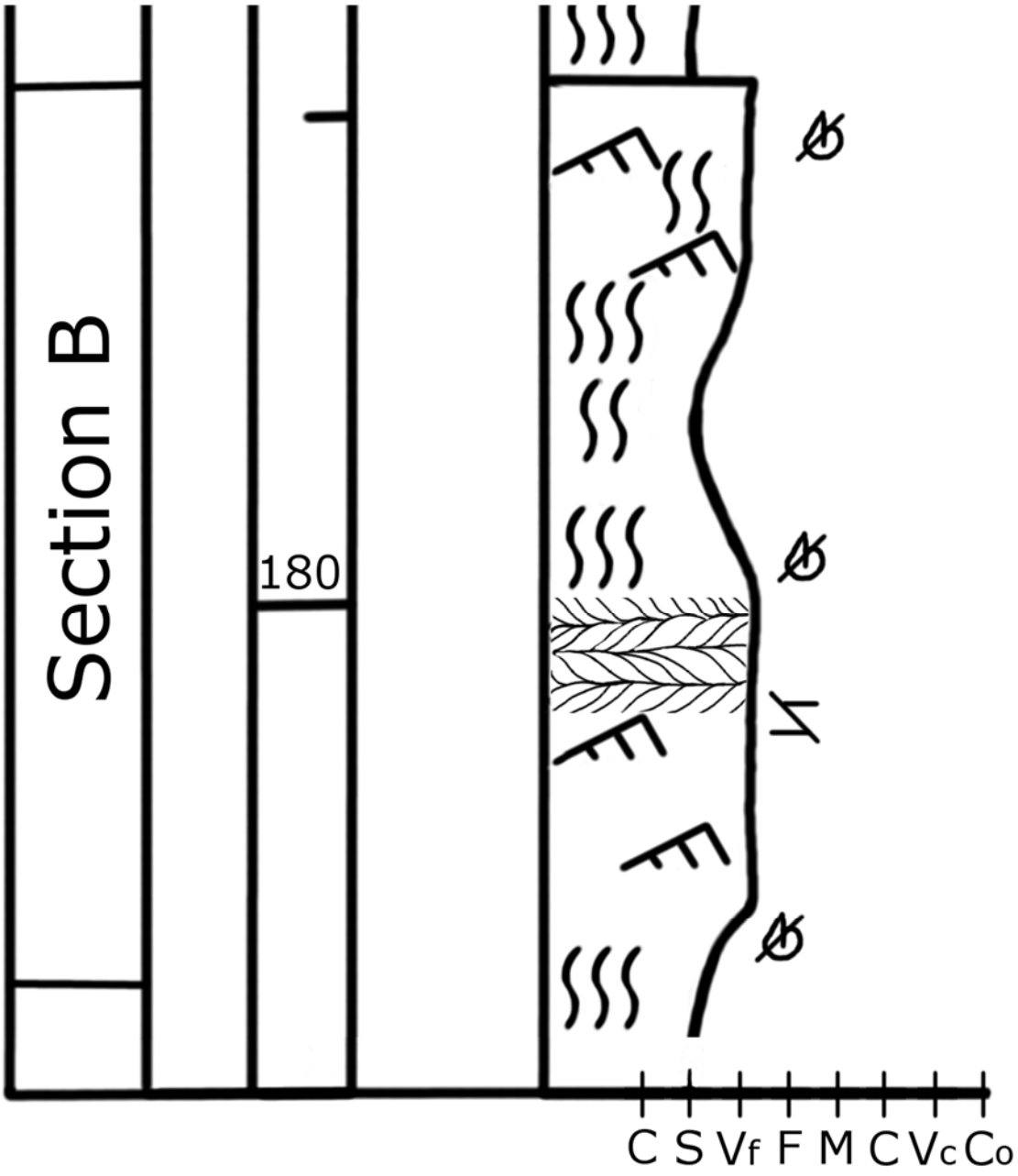

Figure 29: Crop of 7517/12-U-01 Section B

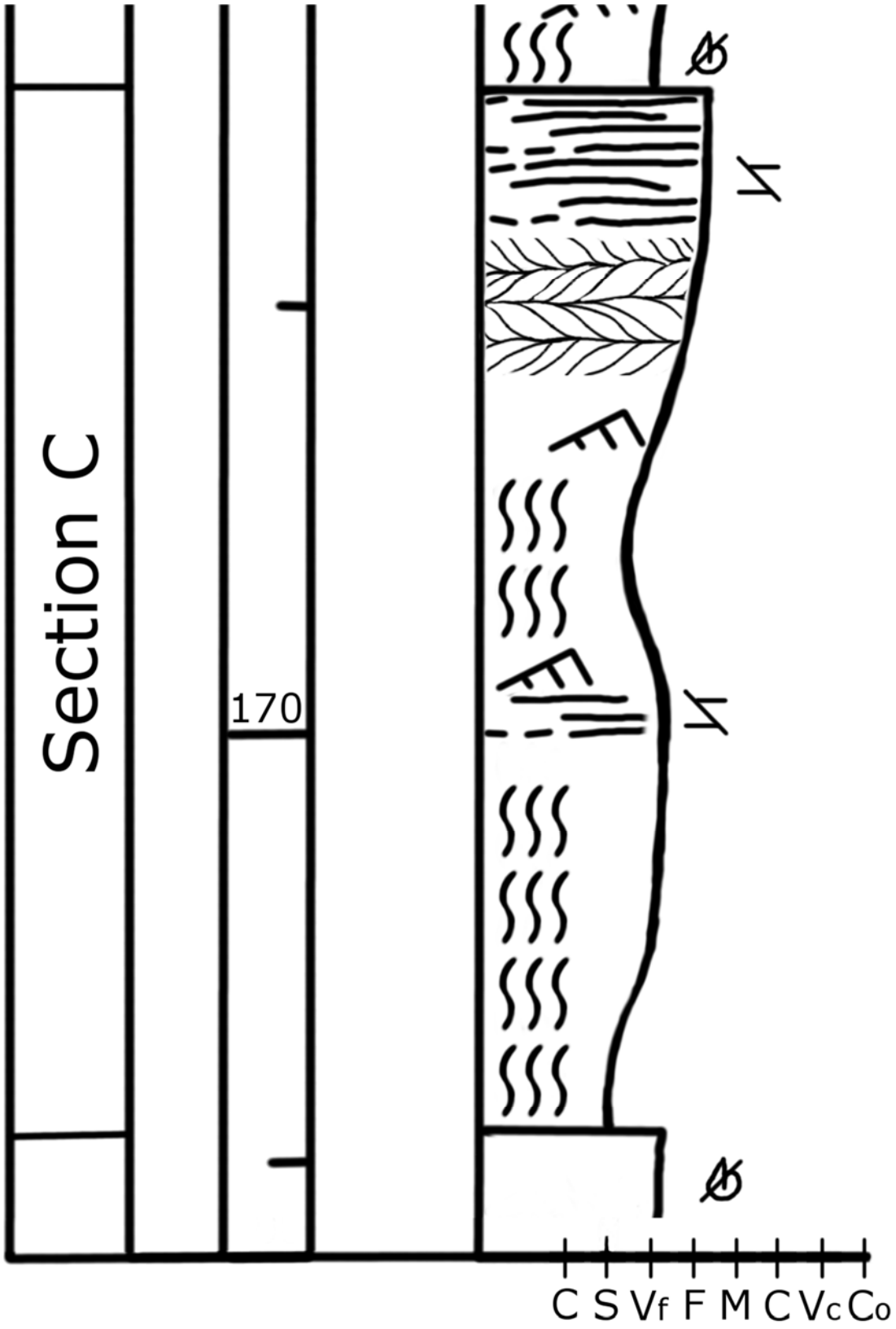

Figure 30: Crop of 7517/12-U-01 Section C

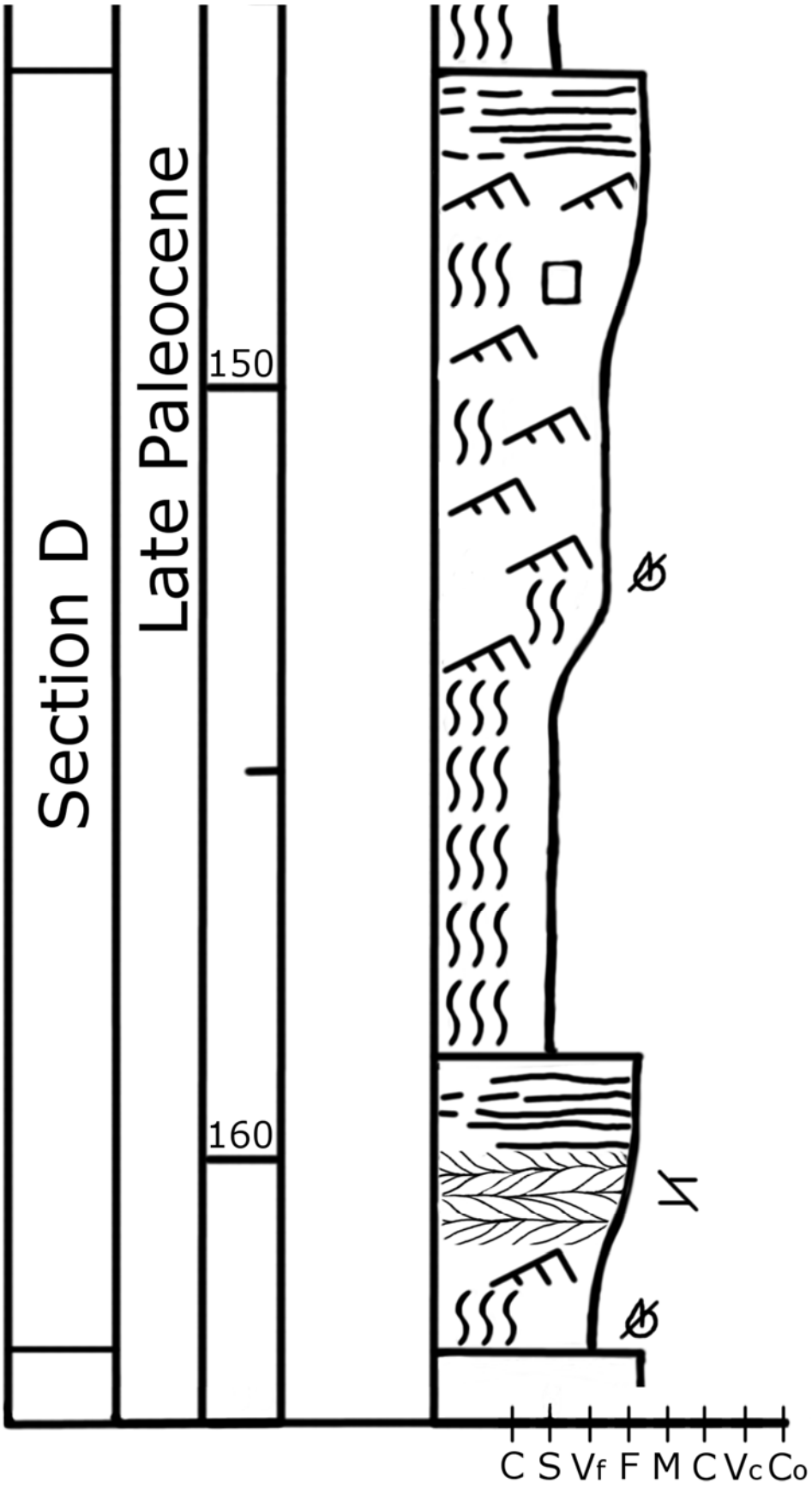

Figure 31: Crop of 7517/12-U-01 Section D

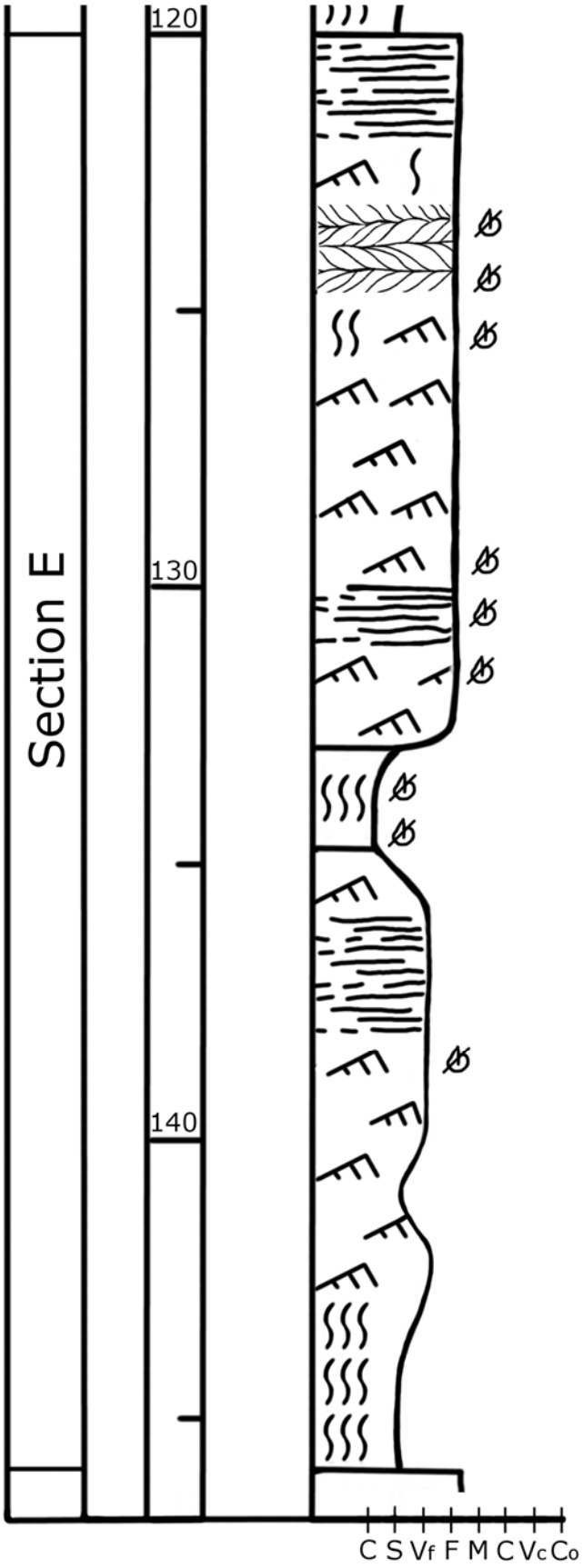

Figure 32: Crop of 7517/12-U-01 Section E

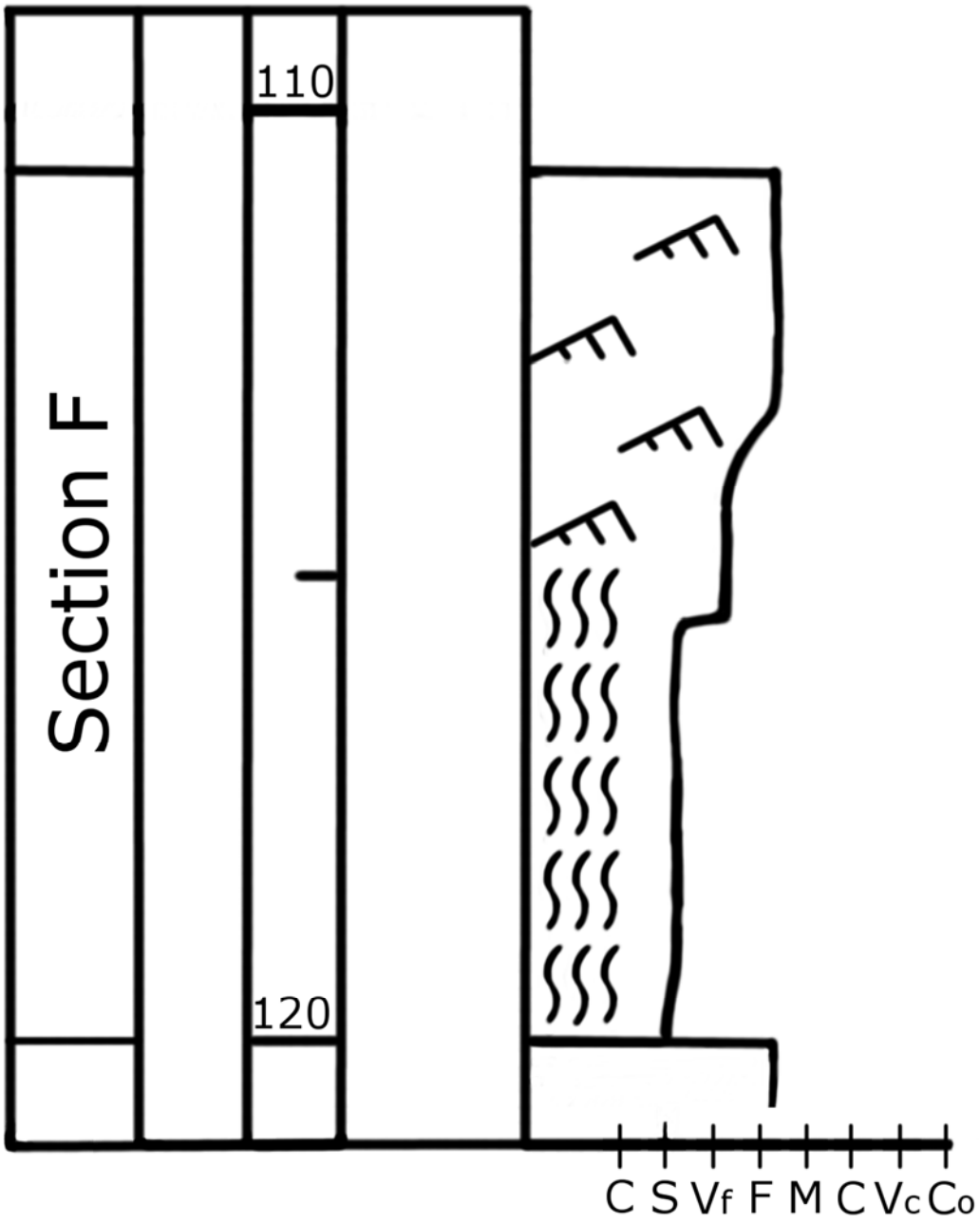

Figure 33: Crop of 7517/12-U-01 Section F

5.2.1.1 Section A 200m-184m

The lowermost section of this core starts at 200m and stretches to 184m, where there is a change in the grain size and colour of the core. The dominating lithology of this section is siltstone. Some intervals within the section occurs, where there is upwards coarsening from silt to fine grained sandstone. The first of these intervals starts at 193m and stretches to 190.6m, and the second interval starts at 189m and ends at 187.5m. A third coarsening upwards section starts at 196m and stretches to 195m, coarsening upward from silt to very fine sand. These coarsening upwards segments creates a funnel shape. Section A consists of mainly dark coloured siltstone

interlaid with lighter coloured coarser sandstones. The siltstones are generally dark grey to black in colour, while the lighter and coarser sandstones are generally very light grey to white in colour.

Some moderate reddish brown intervals are observed between layers or protruding from cracks in the rocks.

Most of the section contains horizontal strata of darker and lighter layers. The sediments have however been heavily reworked and the boundaries between the layers are therefore often destroyed or obscured. This makes it difficult to identify layer boundaries for large parts of the section. Most boundaries seem to be sharp, however some gradual boundaries do occur.

The mudstone layers do not reveal any primary sedimentary structures, while some cross lamination and horizontal layering can be seen in the coarser lighter coloured sandstones.

A lot of cracking of the core do occur in this section, suggesting that the sediments are poorly consolidated.

5.2.1.2 Section B 184m-174.8m

Section B is defined from 184m to 174.8m. The upper boundary is set to 174.8m where there is a noticeable change in lithology. The dominating lithology of this section is very fine-grained sandstone. Some intervals in this section are reworked and darker in colour, and these intervals are higher in silt content. The lighter coloured intervals are very light grey to white in colour, while the darker intervals are dark grey to black with light bluish grey interbedded layers.

This section starts with an upwards coarsening from silt to very-fine sand at 184m to 183m, and then upwards fining at 180m to 178.8m, creating a block shape. Following the block there is 80cm of siltstone before an upwards coarsening interval from 178m to 176.5m. The segment then terminates in a sharp boundary to the next section creating a funnel shape.

The primary sedimentary structures in this section are confined to the coarser sandstone layers. Herringbone cross-lamination and cross-lamination can be seen in these intervals. The darker more fine-grained intervals are reworked and distorted, so no primary structures can be identified.

Layer boundaries are usually sharp, although gradual boundaries do occur. Boundaries between the interbedded layers in silty intervals are usually so reworked that the properties cannot be identified. At 181.9m, there is a displacement of a few mm, as shown in Figure 34.

Figure 34: Displacement from core 7517/12-U-01 at 181.9mRKB

5.2.1.3 Section C 174.8m-162.5m

Section C is defined from 174.8m to 162.5m. At 162.5m, there is a sharp boundary and a change in lithology. The dominating lithology is very light grey to white coloured sandstone. Large intervals of this section is reworked. The reworked intervals are usually dominated by darker sedimentary rocks ranging in colour from light grey to black, with very light grey to white interbedded layers. The reworked parts of the section are most intense in the lower parts and get less intense towards the top of the section.

The section contains a segment that coarsens up from silt to very fine sand, from 174m to 172m and fines up again from very fine sand to silt at 169m to 168m, creating a block shape. At 168m there is a coarsening upwards sequence that goes from silt to fine sand at 162.5m, creating a funnel shape.

Primary sedimentary structures can only be seen in coarser sand layers. There are less intervals with primary structures in the block shape than in the funnel shape. The funnel shape is less reworked and horizontal lamination, herringbone- and cross-lamination can be seen in the sandstones.

Layer boundaries in this section are mostly sharp, although several gradual boundaries can be found. Most of the gradual boundaries are gradual from the bottom towards the top.

At 162.9m a discolouration of the rocks can be seen. The discolouration is a greyish orange and spans an interval of 12cm.

5.2.1.4 Section D 162.5-146m

The fourth section of this core is defined from 162.5m to 146m where there is a sharp boundary and change in lithology from fine sand to silt. The dominating lithology of this section is a very light grey to white coloured sandstone. Some reworked intervals are seen throughout the section, but with an increased occurrence in a finer grained interval from 158.7m to 154m. The reworked intervals are generally interbedded with very light grey to white sandstone and medium light grey siltstone. In one interval between 155.6m to 154m the silty layers are however a bit darker in colour ranging from dark grey to black.

This section contains two coarsening upwards segments between 160m and 158.7m and between 154m and 148.3m, creating two funnel shapes. The lower coarsening upwards segment coarsens from very fine sand to fine sand and the top coarsening upwards segment coarsens from silt to fine sand.

Primary sedimentary structures are confined to the funnel segments where there are less reworking. The structures are horizontal-, herringbone- and cross-lamination, with horizontal lamination being more prevalent in the coarser parts of the funnel.

At 160.9m there is a displacement. The displacement is shown in Figure 35.

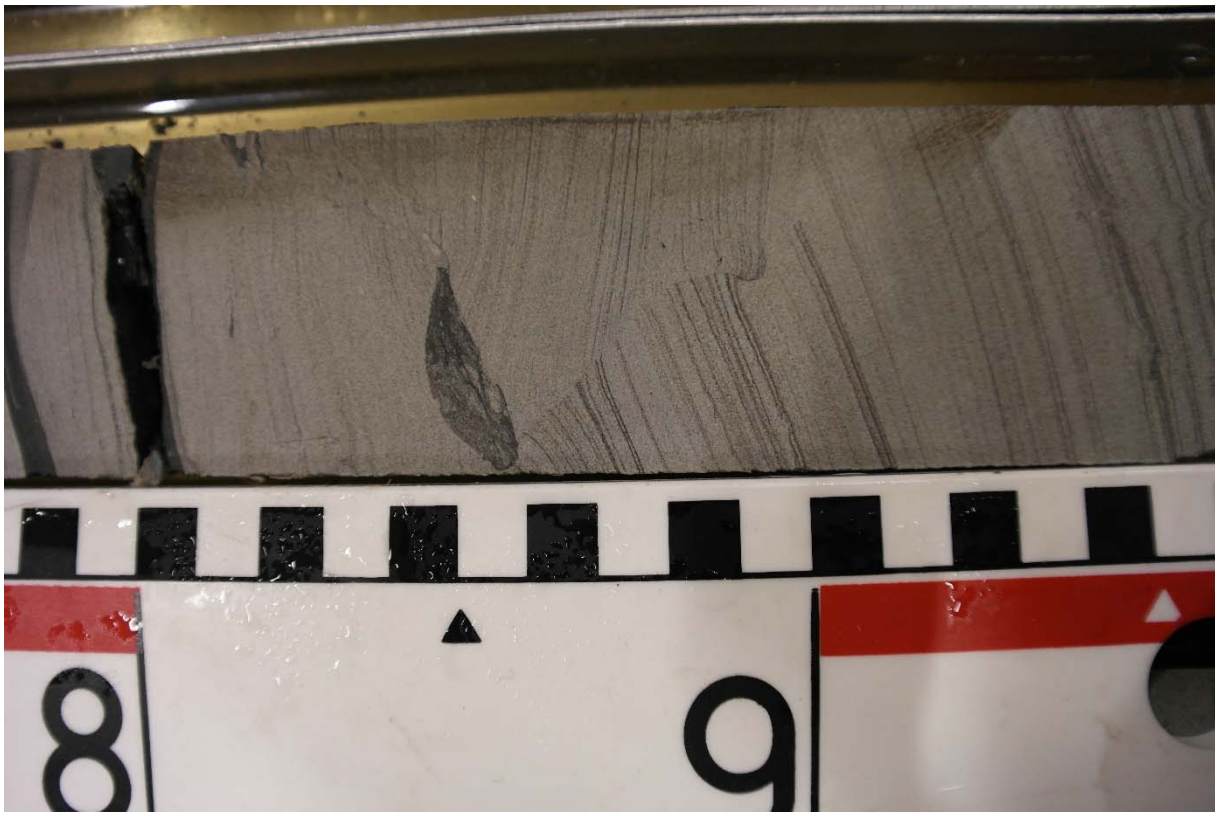

Figure 35: Displacement from core 7517/12-U-01 at 160.9m.

5.2.1.5 Section E 146m-120m

The fifth section of this core starts at 146m and stretches to 120m where there is a sharp transition from fine sand to silt. This section consists of mainly very light grey to white sandstones. The other main lithology of this section is reworked finer grained and darker siltstones. The reworked intervals are interbedded layers of the very light grey to white sandstone and layers of medium to medium light grey siltstone.

In this section, there is a block shape which starts at 144m with a coarsening upwards segment to 142m, where a fining upwards segment starts and stretches to 141m. The change in grain size is from silt to very fine sand, and back to silt again. From 141m to 140m an upwards coarsening segment starts again from silt to very fine sand. At 136m to 134.8m there is an upwards fining segment which ends the block shape. At 133m an upwards coarsening segment starts which stretches to 132.7m, and changes from silt to medium sand. This creates a funnel shape from 133m to 120m.

As seen in the older Sections A to D, the finer grained siltstones intervals are reworked making it difficult to determine primary sedimentary structures. In the block and funnel shaped segments, where we find coarser sands, primary structure can however be observed. The

dominating structure is cross-lamination, with horizontal lamination being the other observed structure. Glauconite can be observed at several interval in the section at, 120.5m, 121.4m, 122.4m, 125.8m, 126.5m and 127.5m.

5.2.1.6 Section F 120m-110.75m

The sixth section of this section starts at 146m and stretches to 110.75m where the core ends. The lower part of this section is mainly reworked siltstone of dark grey to medium grey colour interbedded with very light grey to white coloured sandstone, while the upper part of this segment is a very light grey to white coloured sandstone. The lower part of this section stretches from 120m to 115.4m.

At 115.4m an upwards coarsening segment starts, which stretches to 113.3m. The change in grain size goes from silt to fine sand. The upwards coarsening creates a funnel shape in this segment of the section.

Primary structures are not visible in the reworked silty segment, but cross-lamination can be seen in the sandstone. At 112.5m and 113.3m some glauconite occur over a 20-30cm interval.

The boundaries between the layers are mostly sharp although some gradual boundaries do occur. Between the two segments of this section an erosional boundary can be seen, as shown in Figure 36.

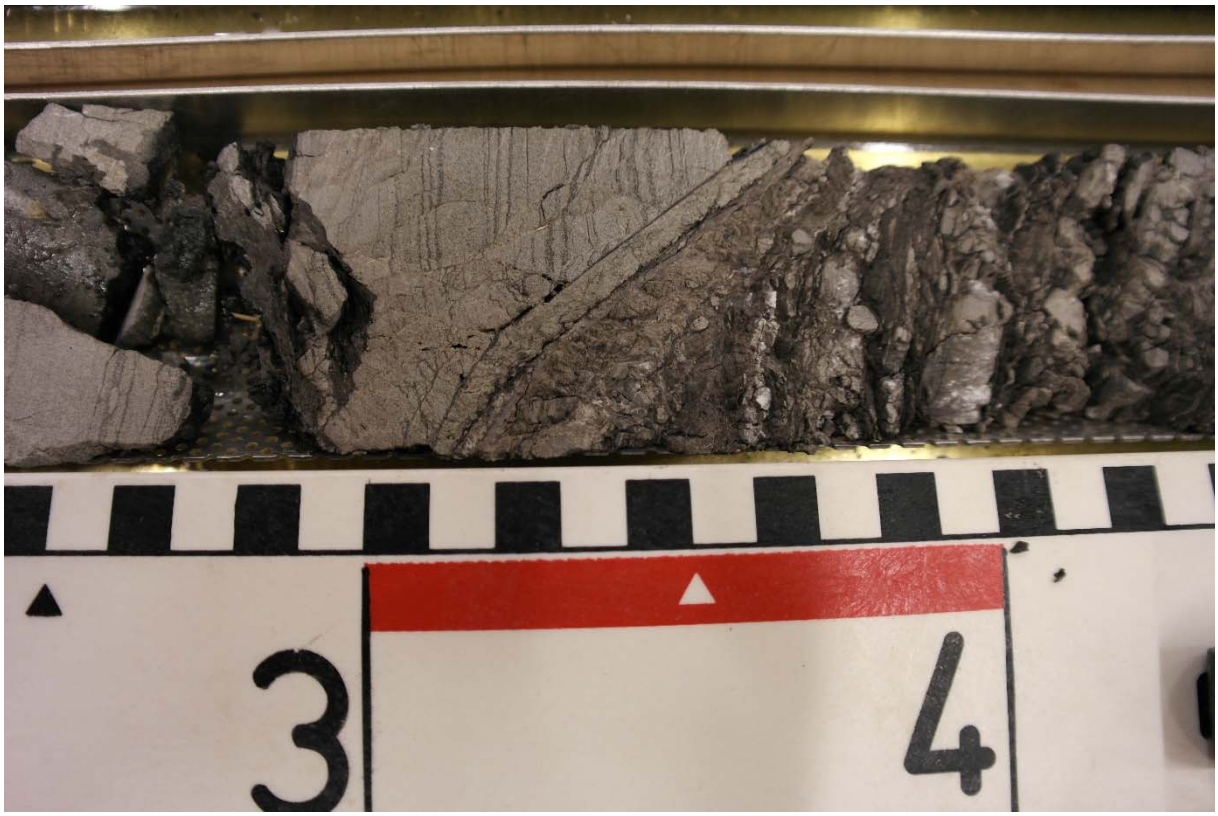

Figure 36: Erosional boundary

5.2.2 Facies Description

5.2.2.1 Upwardscoarsening sandstone

The upwardscoarsening segments of the core consists of light coloured sandstones that gradually coarsens from silt to fine sand. These segments often show some bioturbation in the lower finer grained parts. In the sandier parts of the segment wave ripples followed by herringbone cross-stratification or horizontal lamination can be observed. These segments end in a sharp boundary followed by siltstone successions.

The upwardscoarsening of the segment suggests an increase in environmental energy. The sharp boundary to the following finer grained succession also suggests an abrupt change in environmental energy.

5.2.2.2 Bioturbated Siltstone

These segments consist of siltstones that have been heavily bioturbated. No ichnofacies investigation has been done to this core and so, no distinct bioturbation has been identified. These segments are generally intensely bioturbated to the point where it becomes very difficult to determine primary sedimentary structures.

Fine grained and intensely bioturbated deposits are indicators of low energy environments with low deposition rate (Gingras et al. 2014, Miall 2016).

5.2.2.3 Blocky Sandstone

The blocky sandstone segments are coarseningupwards segments who at the end fines upward instead of abruptly ending in a sharp transition as the upwardscoarsening segments do. These segments follow the same trends as the upwardscoarsening segments, but do also in addition fine upwards. During the upwardsfining segment a shift from horizontal lamination to ripples happen, indicating a decrease in environmental energy (Figure 14).

6 Discussion

6.1 Depositional environment

A depositional environment is defined by a combination of processes giving the depositions identifiable characteristics. In observing and identifying these characteristics an assumption of the paleoenvironment can be made, useful for uncovering the geological history (Nichols 2009). Characteristics of a sedimentary unit that is used to identify the depositional environment are the physical and chemical properties of a rock, lithofacies, the flora and fauna present, biofacies, and trace fossils, ichnofacies. Not all characteristics are always present, or even needed to determine the paleoenvironment. If an environment has an adequately unique characteristic, this alone may be indicative of the paleoenvironment (Nichols 2009). In this thesis, a lithological investigation was done and an ichnofacies description has been done for core 7418/01-U-01 internally in the NPD.

6.1.1 7418/01-U-01

The division into three sections is based mainly on the grain-size distribution of the core. The sections from lowermost to top can be described as dark grey bioturbated siltstone, dark grey bioturbated sandstone and light bluish grey horizontally laminated claystone respectively.

6.1.1.1 Interpretation

The presence of bioturbation in this core suggests deposition in water. The grain size distribution of the core reflects the hydraulic energy of the environment, and the low energy conditions during the deposit of the successions in this core excludes any moving bodies of water, like rivers. The ichnofacies observed suggests that the sediments were not deposited in lacustrine conditions, suggesting the marine as the depositional environment (Collinson et al. 2006, MacEachern et al. 2010, Miall 2016). Further, the dominance of mud reflects deposition from suspension (Ryseth et al. 2003, Miall 2016). Given the slow settling rate of muds deposition away from the coastal processes is likely. Among deep-water processes, there are three main categories, resedimentation, bottom currents and pelagic settling. All of these processes can deposit fine-grained sediments, but among these, resedimentation processes like turbidite flows, happen over a relatively short time span, and therefore give little room for bioturbation. Considering that the succession is abundant in bioturbation, it is unlikely that the succession are derived from resedimentation. There is also the matter of scale to consider, as mass movements are limited in extent. The typical scale of fine-grained turbidites are some centimetres to some tens of centimetres (Stow et al. 1984). This would mean that the succession

consists of several repeating turbidites. Although not all turbidites contain a complete turbidite sequence, the lower erosional boundary would be expected to be present, and there are few erosional boundaries observed in the succession (Stow et al. 1984). Sedimentary deposits affected by bottom currents are called contourites. Both contourites and pelagic sedimentation happens on a larger scale than turbidites, and fit better with the observed succession. Distinguishing between fine sediment contourites and pelagites can be difficult as both generally have a slow sedimentation rate, allowing for intense bioturbation. Contourites are affected by bottom currents and therefore can display some primary sedimentary structures, but this is not a given (Stow et al. 1984). When comparing the proposed facies models for contourites, pelagic and hemipelagic sequences from Stow et al. (1984) (Figure 37), there is little difference between these, and determining the exact depositional process is therefore difficult. The observed trace fossils, *Chondrites*, *Planolites* and *Lophoctenium* are diagnostic for pelagic deposits, and may indicate that the succession is of pelagic or hemipelagic origin (Stow et al. 1984).

The transition into the coarser section B, indicate a shift to a higher energy environment (Figure 13). The transition to a higher energy environment indicates a shallowing of the local water level at the site of the core, bringing the coast, where higher energy processes occur, closer to the site. This can be caused by a change in sea level or progradation of sediments causing the relative sea level to fall. Commonly, with prograding coastlines, there is a gradual coarsening upwards sequence, however the transition from sequence A to sequence B is erosional, with a conglomerate marking the transition (5.1.1.1, Figure 25). Plint (1988) describes a similar succession where the transition to coarser grained sediments in some areas of a formation is sharp based, appropriately called sharp-based sandstone bodies (Plint 1988, Miall 2016). These sand bodies occur when the relative sea level fall exceeds the rate of basin subsidence. This allows for the fair-weather wave base (FWWB) to reach the otherwise untouched deeper muds, creating an erosional surface, which then the sandy layers are deposited on top of (Figure 38) (Plint 1988).

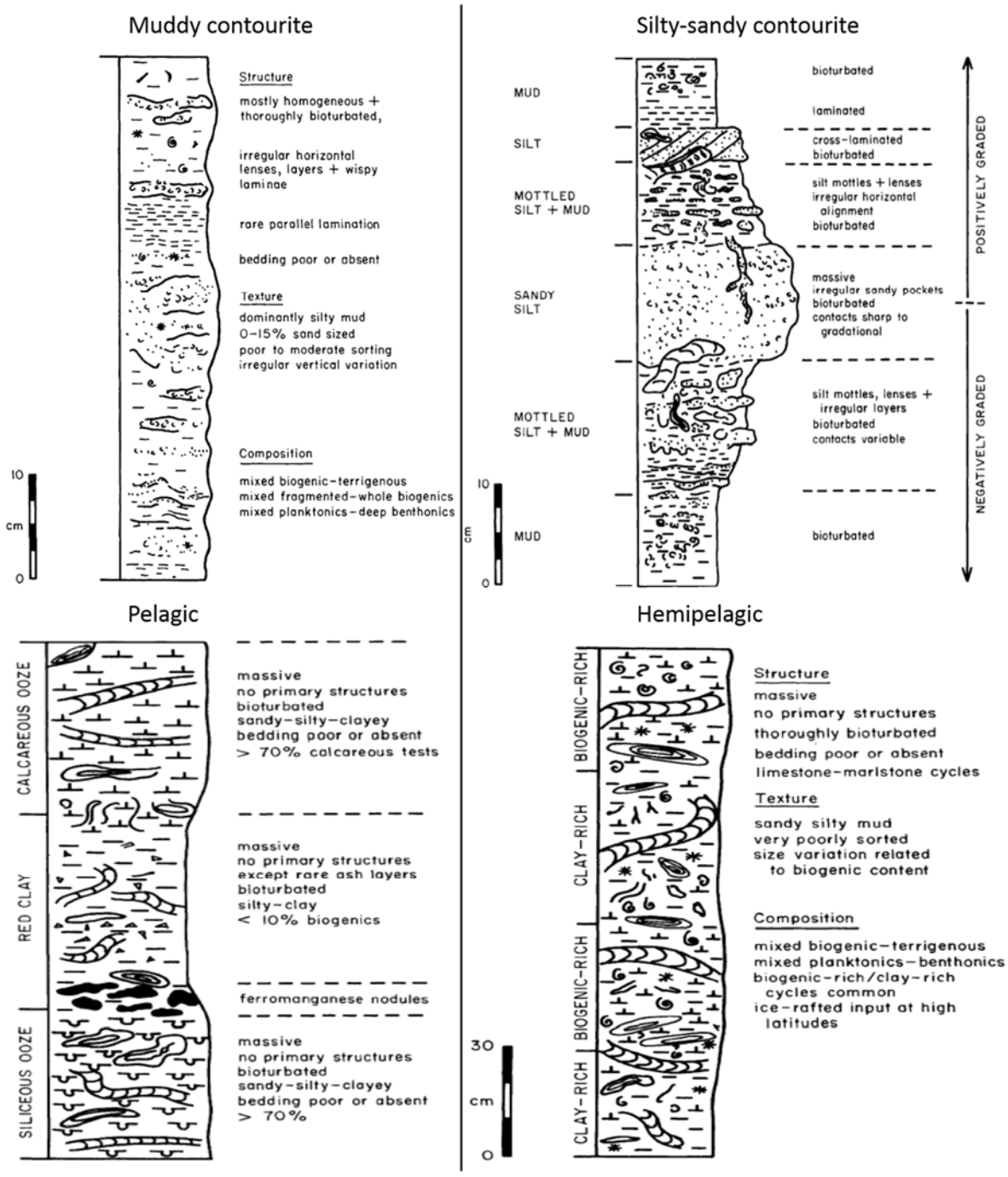

Figure 37: Facies models for contourites pelagic and hemipelagic sequences proposed by Stow et al. (1984)

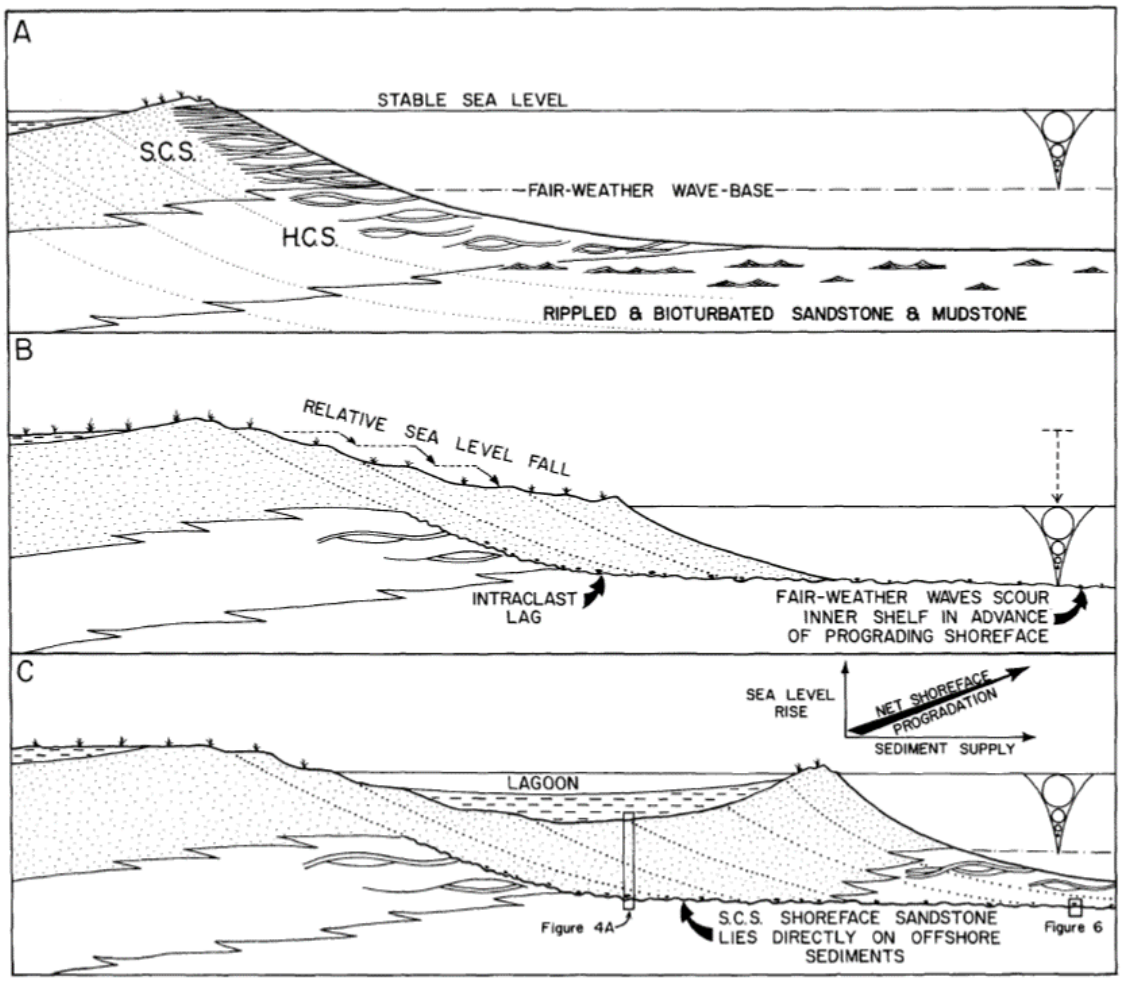

Figure 38: Diagram showing the formation of sharp-based sand bodies. A shows a stable situation where the offshore succession is below the FWWB, and thus not affected much by wave dominated processes. B show the rapid fall in sea level causing the FWWB to reach the offshore sediments causing erosion of the surface. C shows the sand body resting atop the erosional surface. (Plint 1988)

The transition from section B to section C is also erosional and marked by a conglomerate (5.1.1.2, Figure 26). The transition is from sandstones to claystones indicating an offshore environment again. This change in depositional environment suggests a transgressive event and relative rise in sea level. The low intensity of bioturbation suggests that there either were a high sedimentation rate and low food source, and/or low oxygen conditions. The lack of any primary structures and the fine-grained composition of the section indicates that the depositional environment was very low energy. Little water circulation can lead to little exchange of water masses and oxygen depletion, explaining the low amounts of bioturbation.

Combining the observed information about the core, the depositional environment is suggested in FigX. The transition from section A to section B and section B to section C represent regressive and transgressive events respectively.

6.1.2 7517/12-U-01

This core, unlike the other, cannot easily be divided into easily observed sections. However, by simplifying the observed log three distinct facies can be observed throughout the core. The three facies are bioturbated siltstone, upwardscoarsening sandstones and blocky sandtones. In the described sections, two or all of these facies can be found.

6.1.2.1 Interpretation

The presence of bioturbation in this core suggests deposition in a water.

The energy of the depositional environment is reflected in grain size distribution, as larger grains demand more energy to move (Miall 2016). The relatively fine-grained composition of this core indicates a low deposition environment, excluding moving bodies of water. Intense bioturbation indicates marine conditions, as lake water stratification often creates anaerobic conditions on the lake floor, making it unsuitable for life (Nichols 2009).

The intense bioturbation of large parts of the core is an indicator of exchange of water masses through water circulation, and therefore suggests a more dynamic marine setting rather than the staler lacustrine lakes. This is further supported by the presence of glauconite, a mineral commonly found in marine sediments (Nichols 2009, Miall 2016).

Section A, is dominated mainly by intensely bioturbated siltstone (Figure 28). Some horizontal layering is visible but most is obscured by the bioturbation. The bioturbated siltstone facies suggests a low energy low deposition environment. The coarsening upwards sequence in the section indicates an increase in energy at the location, and the decreasing amount of bioturbation indicates a higher sediment supply (Gingras et al. 2014).

Section B shows a longer upwardscoarsening sequence (Figure 29). Within the upwardscoarsening sequence the primary structures goes from ripples to herringbone cross-lamination. Herringbone cross-stratification is associated with tide-dominated seas, but are not exclusive to it (Nichols 2009, Miall 2016).

The first sequence in section C shows a blocky sandstone facies, where there is initially a coarsening-upwards sequence, followed by a fining-upwards sequence. The primary structures follow the same observed trend where horizontal lamination represents the highest energy interval while ripples and bioturbation represent lower energy environments. Within both

horizontal lamination intervals, there are displacements, indicating tectonization (Figure 34). In the upwardscoarsening sequence the sedimentary structures changes from ripples to lamination, indicating a shift from lower to higher energy according to the Hjülstrom diagram (Figure 13).

By section E, the bioturbated silt beds become less prevalent and the sandstones begin to dominate the succession. This marks a shift to a higher energy environment. Some changes in energy can still be observed in the change in primary structures from ripples to horizontal lamination and back again. Towards the end of the section, glauconite becomes prevalent in the sediments, giving them a green colour. The presence of glauconite limits the water depth at which deposition happened, as glauconite typically only occur at depth of 50m-500m. It also suggests that at the time the sedimentation rates were slow as it most commonly occur under conditions where sedimentation of other material is slow. This is significant as outer shelf sedimentation tends to be slowest during periods of sea level rise (Nichols 2009).

The entire core consists of several coarseningupwards sequences with sequences of bioturbated silt. The coarseningupwards sequences become more frequent and massive towards the top of the core. This indicates that the hydraulic energy of the environment gradually becomes higher, in addition to the individual episodes of higher energy represented by the coarseningupwards sequences. The presence of ripples and horizontal lamination together with the sandy lithology suggests a shallow marine environment (Nichols 2009). The herringbone cross-stratification is usually associated with tide-dominated environments, although it may appear in other settings as well (Nichols 2009, Miall 2016).

Combining the observed information about the core, the depositional environment is suggested in FigX. One depositional environment is recognized, but distinguished between low and high energy.

.

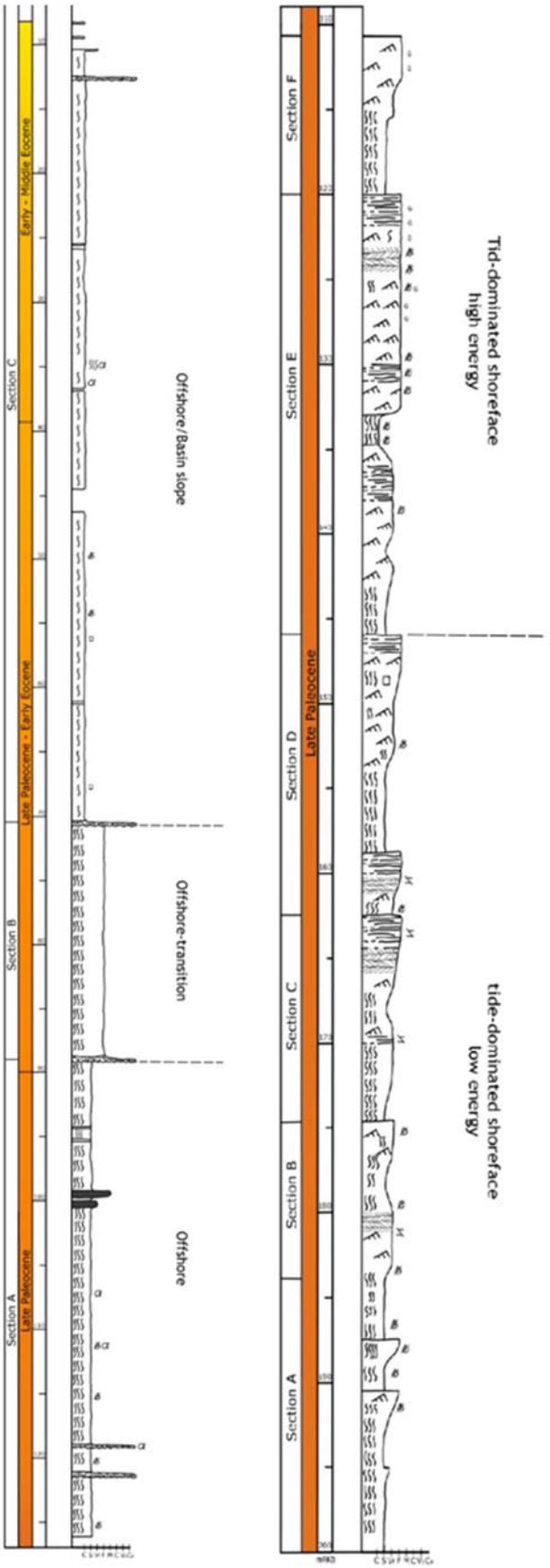

Figure 39: Core 7418/01-U-01 and 7517/12-U-01 with interpreted depositional environments

6.2 Regional Setting

6.2.1 Paleocene

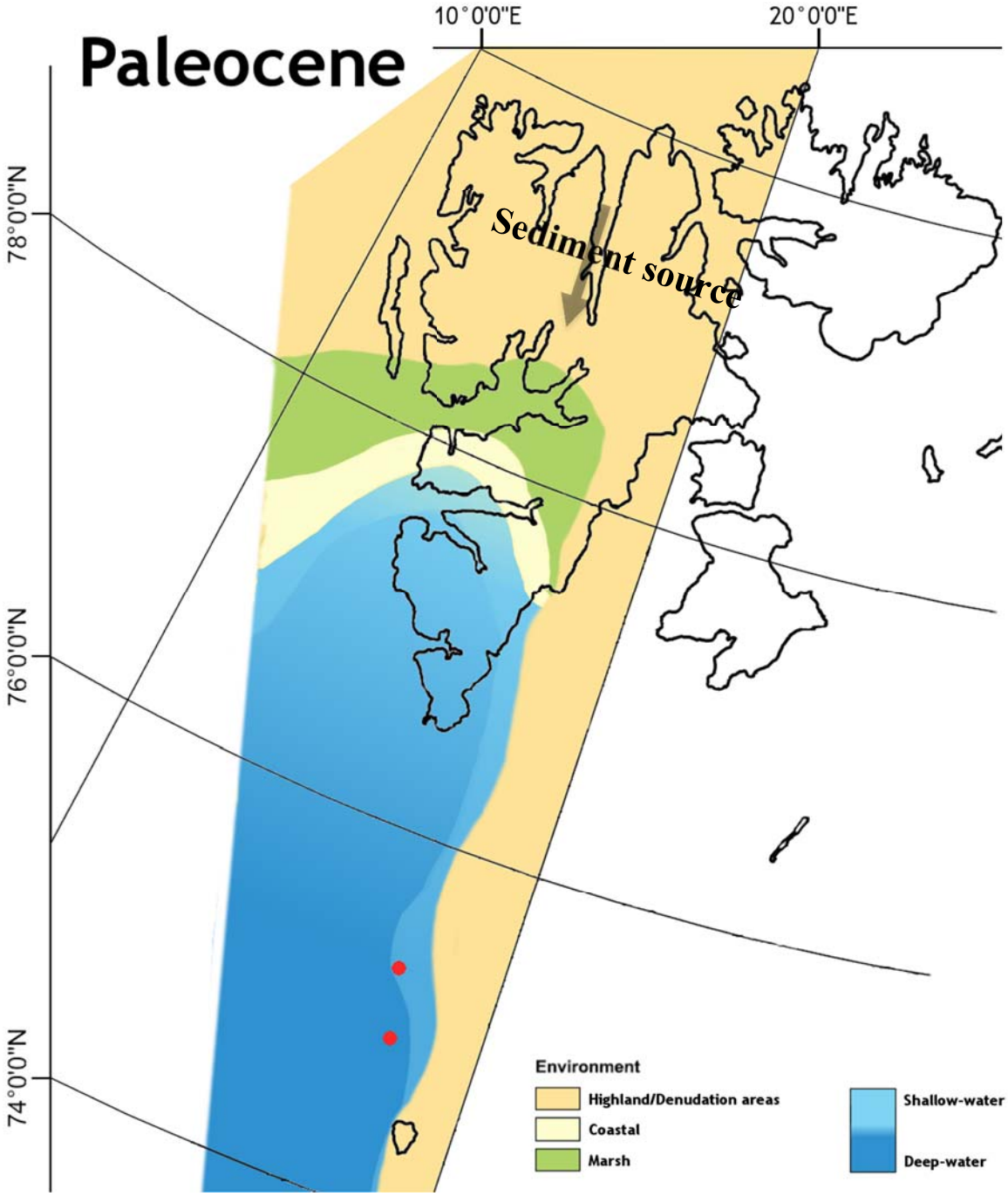

Figure 40: Proposed paleomap of the NW Barents Sea during Paleocene. The map is based in part on Petersen et al. (2016), who suggested the sediment source area in Paleocene to be from the northeast. The results from this study is worked into that model

The Paleocene succession is present in both core analysed. The southern 7418/01-U-01 is interpreted to represent deep-marine conditions at the time of deposition during Paleocene. The

northern core 7517/12-U-01 shows coarser lithology, believed to represent shallow-marine conditions.

The Late Paleocene succession from well 7216/11-1S from the Sørvestnaget Basin is described by Ryseth et al. (2003) as greyish mudrocks with traces of very fine-grained to fine-grained sandstone, and varicoloured red, grey, greenish to blackish mudrocks. The interpretation is deposition in a low energy marine environment.

6.2.2 Eocene

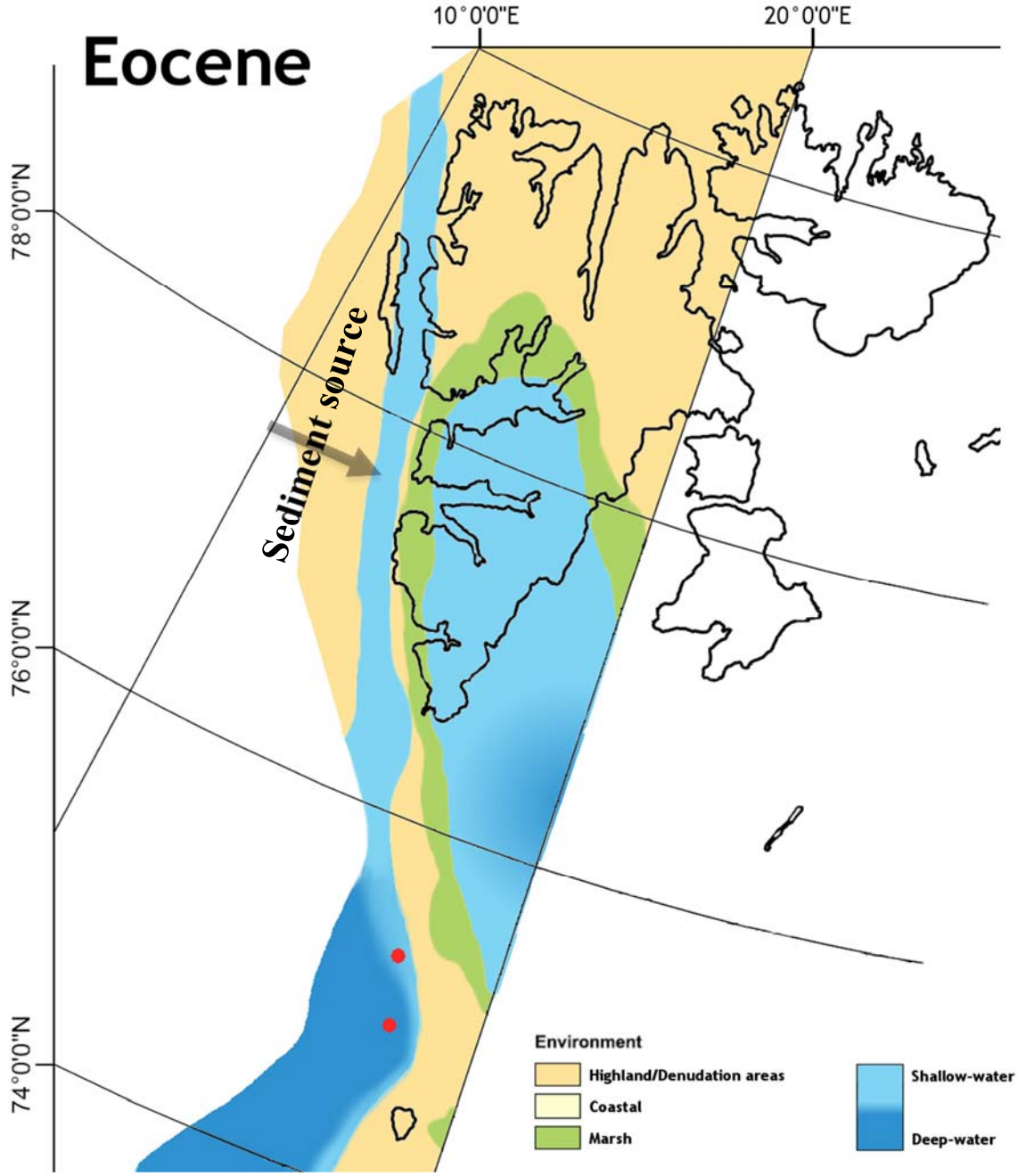

Figure 41: Proposed paleomap of the NW Barents Sea during Eocene. The Map is based on Smelror et al. (2009) and Petersen et al. (2016) has been reworked to fit with this study's findings.

7 Conclusion and summary

Through the description and interpretation of the two shallow cores of this project some observations have been made.

- The Eocene succession is not present at the site of borehole 7517/12-U-01

- Core 7418/01-U-01 consists of three different sections which all represent different depositional facies. These sections are all deposited in deep marine conditions and the transitions between these sections represent a regressive and a transgressive episode.

- Core 7517/12-U-01 was deposited in shallow marine conditions and consists several upwardscoarsening section, which make up one long regressive event.

- Core 7418/01-U-01 show similarities to the Paleocene and Eocene successions to the south in the Sørvestnaget Basin

- Core 7517/12-U-01 show similarities to its contemporary deposits at the Central Basin, Svalbard.

8 Refrences

Works cited. "Faktasider Oljedirektoratet." Retrieved 2017-03-19, from http://factpages.npd.no/FactPages/default.aspx?nav1=wellbore&nav2=PageView|Other|OtherAll&nav3=2185&culture=en.

(2008) SINTEF. IKU Stratigraphic Drilling Projects 1982 - 1993

Andersen, M. and J. Aars (2016). "Barents Sea Polar Bears (Ursus Maritimus): Population Biology And Anthropogenic Threats." Polar Research **35**.

Anell, I., et al. (2016). "Regional tectono-sedimentary development of the highs and basins of the northwestern Barents Shelf." Norwegian Journal of Geology **96**(1): 27-41.

Bergh, S. G. and P. Grogan (2003). "Tertiary structure of the Sørkapp-Hornsund Region, South Spitsbergen, and implications for the offshore southern extension of the fold-thrust Belt." Norwegian Journal of Geology **83**: 43-60.

Blinova, M., et al. (2009). "Structure and evolution of the Bellsund Graben between Forlandsundet and Bellsund (Spitsbergen) based on marine seismic data." Norwegian Journal of Geology **89**: 215-228.

Brekke, H., et al. (2001). "Sedimentary Environments Offshore Norway - Paleozoic to Recent." Norwegian Petroleum Society Special Publications **10**: 7-37.

Brown, A. R. (1999). Interpretation of three-dimensional seismic data (5th ed.), American Association of Petroleum Geologists.

Bugge, T. and S. Fanavoll (1995). "The Svalis Dome, Barents Sea-a geological playground for shallow stratigraphic drilling." First Break **13**(6): 237-251.

Collinson, J., et al. (2006). Sedimentary Structures third edition. United Kingdom, Terra Publishing.

Czuba, W. (2014). Continental Passive Margin West of Svalbard and Barents Sea in Polish Arctic Seismic Studies. Achievements, History and Challenges in Geophysics. R. M. Bialik, M.; Moskalik, M., Springer International Publishing**:** 234-252.

Dalland, A., et al. (1988). A lithostrategraphic scheme for the Mesozoic and Cenozoic succession offshore mid- and northern Norway. NPD Bulletin. **4**.

Doré, A. G. (1995). "Barents Sea Geology, Petroleum Resources and Commercial Potential." Arctic **48**(3): 207-221.

Droser, M. L. and D. J. Bottjer (1986). "A Semiquantitative Field Classification Of Ichnofabric." Journal of Sedimentary Petrology **56**: 558-559.

Eidvin, T. E., et al. (1998). "The Pleistocene to Middle Eocene stratigraphy and geological evolution of the western Barents Sea continental margin at well site 7316/5-1 (Bjørnøya West area)." Norsk Geologisk Tidsskrift **78**: 99-123.

Eldholm, O., et al. (1987). "Continent-ocean transition at the western Barents Sea/Svalbard continental margin." Geology **15**: 1118-1122.

Evenset, A., et al. (2004). "A comparison of organic contaminants in two high Arctic lake ecosystems, Bjørnøya (Bear Island), Norway." The Science of the Total Environment **318**: 125-141.

Faleide, J. I., et al. (1996). "Late Cenozoic evolution of the western Barents Sea-Svalbard continental margin." Global and Planetary Change **12**: 53-74.

Faleide, J. I., et al. (2008). "Structure and evolution of the continental margin off Norway and the Barents Sea." Episodes 2008 **31**: 82-91.

Faleide, J. I., et al. (1993). "Late Mesozoic-Cenozoic evolution of the south-western Barents Sea in a regional rift-shear tectonic setting." Marine and Petroleum Geology **10**: 186-214.

Gabrielsen, R. H. (1984). "Long-lived fault zones and their influence on the tectonic development of the southwestern Barents Sea." Journal Of The Geological Society **141**(4): 651-662.

Gabrielsen, R. H., et al. (1990). Structural Elements of The Norwegian Continental Shelf. Part I: The Barents Sea Region. NPD-Bulletin. **6:** 33.

Gingras, M. K. and S. G. Pemberton (2014). "Bioturbation: Reworking Sediments for Better or Worse." Oilfield Review **26**(4): 46-58.

Grogan, P., et al. (1999). "Structural elements and petroleum geology of the Norwegian sector of the northern Barents Sea." Petroleum Geology: 247-259.

Henriksen, E., et al. (2011). Uplift and erosion of the greater Barents Sea: impact on prospectivity and petroleum systems. Arctic Petroleum Geology. A. M. E. Spencer, A. F.; Gautier, D. L.; Stoupakova, A. V.;Sørensen, K., Geological Society of London**:** 271-281.

Livšic, J. J. (1992). "Tectonic history of Tertiary sedimentation of Svalbard." Norsk Geologisk Tidsskrift **72**: 121-127.

MacEachern, J. A., et al. (2010). Ichnology and Facies Models. Facies Models 4. N. P. James and R. W. Dalrymple. Canada, Geological Association of Canada**:** 19-58.

Martens, I. (2016). Different geological methods operate at different scales and phases. Lecture notes.

Miall, A. D. (2016). Stratigraphy: A Modern Synthesis. Switzerland, Springer.

Myhre, A. M., et al. (1982). "The margin between Senja and Spitsbergen fracture zones: Implications from plate tectonics." Tectonophysics **89**: 33-50.

Nichols, G. (2009). Sedimentology and Stratigraphy second edition, Wiley-Blackwell.

NPD (2017). FactPages. NPD.

Petersen, T. G., et al. (2016). "Provenance shifts in an evolving Eurekan foreland basin: the Tertiary Central Basin, Spitsbergen." Journal Of The Geological Society **173**: 634-648.

Plint, A. G. (1988). "Sharp-Based Shoreface Sequences and "Offshore Bars" In The Cardium Formation Of Alberta: Their Relationship To Relative Changes In Sea Level." SEPM Special Publications **42**: 357-370.

Rider, M. and M. Kennedy (2011). The geological interpretation of well logs, third edition, Rider-French Consulting Ltd.

Riis, F., et al. (2008). "Evolution of the Triassic shelf in the northern Barents Sea region." Polar Research **27**: 318 - 338.

Rise, L. and J. Sættem (1994). "Shallow stratigraphic wireline coring in bedrock offshore Norway." Scientific Drilling **4**: 243-257.

Ritzmann, O. and W. Jokat (2003). "Crustal structure of northwestern Svalbard and the adjacent Yermak Plateau: evidence for Oligocene detachment tectonics and non-volcanic breakup." Geophys J Int **152**: 139-159.

Ritzmann, O., et al. (2002). "Crustal structure between the Knipovich Ridge and the Van Mijenfjorden (Svalbard)." Marine Geophysical Researches **23**: 379-401.

Ryseth, A., et al. (2003). "Cenozoic stratigraphy and evolution of the Sørvestnaget Basin, southwestern Barents Sea." Norwegian Journal of Geology **83**: 107-130.

Selley, R. C. and S. A. Sonnenberg (2015). Elements of petroleum Geology, Third edition, Elsevier.

Sheriff, R. (1980). "Nomogram for Fresnel-zone calculation." Geophysics **45**(5): 968-972.

Skogseid, J., et al. (2000). "NE Atlantic continental rifting and volcanic margin formation." Geological Society, London, Special Publications **167**: 295-326.

Smelror, M., et al. (2009). Geological History of the Barents sea. Trondheim, Norsk Geologisk Undersøkelse.

Steel, R. J. and D. Worsley (1984). Svalbard's post-Caledonian strata - an atlas of sedimentational patterns and palaeogeographic evolution. Petroleum Geology of the North European Margin. A. M. Spencer, Springer Netherlands**:** 109-135.

Stow, D. A. V. and D. J. W. Piper (1984). "Deep-water fine-grained sediments: facies models." Geological Society, London: Special Publications **15**: 611-646.

Sættem, J., et al. (1994). "Cenozoic margin development and erosion of the Barents Sea: Core evidence from southwest of Bjørnøya." Marine Geology **118**: 257-281.

Wood, R. J., et al. (1989). Influence of North Atlantic Tectonics on the Large-Scale Uplift of the Stappen High and Loppa High, Western Barents Shelf. Extensional Tectonics and Stratigraphy of the North Atlantic Margins. A. J. B. Tankard, H. R., American Association of Petroleum GeologistsCanadian Geological Foundation. **46:** 559 - 556.

Worsley, D. (2008). "The post-Caledonian development of Svalbard and the western Barents Sea." Polar Research **27**: 298-317.

Figures

Ayogo blog-patient engagement. (2015, July 16). Retrieved from Ayogo: http://ayogo.com/blog/patient-engagement-definition/6-blind-men-illustration-hans-moller-2/

NPD. (2017, March 19). *FactPages*. Retrieved from NPD: http://factpages.npd.no/FactPages/default.aspx?nav1=wellbore&nav2=PageView|Other|OtherAll&nav3=2185&culture=en

SINTEF. (2008, February 28). Retrieved from IKU Stratigraphic Drilling Projects 1982 - 1993: https://www.sintef.no/projectweb/ik-stratigraphic-drilling/drilling-information/